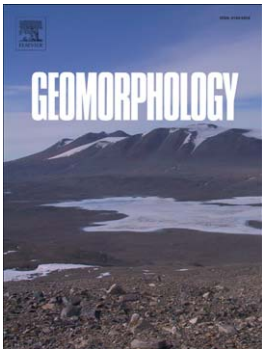

Space-for-time substitution and the evolution of a submarine canyon-channel system in a passive progradational margin

Aaron Micallef, Marta Ribó, Miquel Canals, Pere Puig, Galderic Lastras, Xavier Tubau

PII: S0169-555X(14)00308-0
DOI: doi: 10.1016/j.geomorph.2014.06.008
Reference: GEOMOR 4813

To appear in: *Geomorphology*

Received date: 16 December 2013
Revised date: 3 June 2014
Accepted date: 6 June 2014

Please cite this article as: Micallef, Aaron, Ribó, Marta, Canals, Miquel, Puig, Pere, Lastras, Galderic, Tubau, Xavier, Space-for-time substitution and the evolution of a submarine canyon-channel system in a passive progradational margin, *Geomorphology* (2014), doi: 10.1016/j.geomorph.2014.06.008

Manuscript submitted to Geomorphology:

Space-for-time substitution and the evolution of a submarine canyon-channel system in a passive progradational margin.

Aaron Micallef[a,b]*, Marta Ribó[c], Miquel Canals[a], Pere Puig[c], Galderic Lastras[a], Xavier Tubau[a]

[a] GRC Geociències Marines, Facultat de Geologia, Universitat de Barcelona, E-08028 Barcelona, Spain.

[b] Department of Physics, University of Malta, Msida, MSD 2080, Malta.

[c] Institut de Ciències del Mar, CSIC, Passeig Marítim de la Barceloneta 37–49, E-08003 Barcelona, Spain.

*Corresponding author. Tel: +356 2340 3613.

E-mail address: aaron.micallef@um.edu.mt (A. Micallef)

Abstract

Space-for-time substitution is a concept that has been widely applied, but not thoroughly tested in some fields of geomorphology. The objective of this study is to test whether the concept of space-for-time substitution is valid in reconstructing the evolution of a submarine canyon-channel system in a passive progradational margin. We use multibeam echosounder data and in situ measurements from the south Ebro Margin to analyse the morphology and morphometry of a sequence of submarine valleys ordered in terms of increasing valley thalweg length. The morphological model of submarine valley evolution that we can propose from this analysis is very similar to established models in the literature, which leads us to conclude that time can be substituted by space when reconstructing the evolution of submarine canyon and channel systems in the south Ebro Margin. By extracting morphometric information from the application of the space-for-time substitution model to our data, we identify a series of morphological patterns as a submarine canyon evolves in a passive progradational margin. These include the geometric similarity of canyon planform shape, an increase in canyon draining efficiency and in the influence of flank slope failures, and an evolution towards equilibrium between canyon form and imposed water and sediment load without net erosion or deposition taking place. We also observe that canyon elongation is higher downslope and that the canyon undergoes an early stage of rapid incision similar to the process of "erosion narrowing" reported in terrestrial rivers. We demonstrate that the conclusions of our study are not limited to submarine valleys in the south Ebro Margin but are applicable to other margins around the world.

1. Introduction

Geoscientists are generally unable to fully observe landscape-forming processes because the time-scale of the observer and the time-scale of many geomorphic phenomena are very different. One approach to solve this issue has been to substitute space for time, which is known as the concept of space-for-time substitution. This concept, which has also been applied in ecology, refers to the inference of long-term landform development from the comparison of similar landforms of different ages or at different stages of evolution (Paine, 1985; Pickett, 1989; Li et al., 2011; Fryirs et al., 2012). Space-for-time substitution was initially used to reconstruct drainage basin evolution and sequential slope development (e.g. Glock, 1931; Schumm et al., 1984; Simon and Hupp, 1986). More recently, the concept has been applied to determine how drainage basins evolve towards steady state (Stolar et al., 2007) to identify the erosional and topographic response of drainage basins to tectonic deformation (Hilley and Arrowsmith, 2011), explain the transition from fluvial to glacial landscapes (Kirkbride and Matthews, 1997), reconstruct the evolution of channelled sea cliffs (Leyland and Darby, 2008), infer rates of cliff retreat and talus development (Obanawa et al., 2009), and understand how slope geomorphology and soil change with elevation and precipitation (Huggett, 1998; Schmidt and Meitz, 2000). The application of space-for-time substitution in submarine geomorphology has been sparser and focused almost entirely on submarine canyons. Using side-scan sonar data from the USA Atlantic margin, Twichell and Roberts (1982) and Farre et al. (1983) were able to propose a model of canyon evolution based on the retrogressive failure of the canyon head and walls. In this model, slope-confined canyons, which are considered representative of the immature stages

in canyon development, eventually evolve headwards into mature canyons that breach the shelf break.

Despite its accepted use in the geomorphic literature, the concept of space-for-time-substitution is not well proven. The concept is based on ergodic reasoning, which has been developed in physics to establish the spatial distribution of fast moving molecules (Boltzmann, 1871). According to ergodic reasoning, the mean observation of an individual molecule made over time is equal to the mean observations of many molecules at a single moment in time over an area. Thus, observations made at different times can be used as surrogate for the spatial distribution of molecules at a single moment. In geomorphology, ergodicity has not been applied in the original sense of time and space averages; instead, it is based on the use of space as a surrogate of time and the translation of a spatial morphological sequence into a temporal sequence of individual landform evolution and change (Kirkbride and Matthews, 1997; Leyland and Darby, 2008; Obanawa et al., 2009; Hilley and Arrowsmith, 2011). Distance, location, landform dimension and complexity are used as ergodic indicators of landform development to derive the spatial sequence, which was not intended by the original concept.

The objectives of this paper are: (i) to test whether the concept of space-for-time substitution is valid in submarine geomorphology, specifically in reconstructing the evolution of a submarine canyon-channel system in a passive progradational margin, and (ii) to gain new insights into the morphological evolution of submarine canyon-channel systems. We fulfil these objectives by carrying out morphological, morphometric and allometric analyses of submarine canyons and channels incising the south Ebro Margin, a passive progradational continental margin located in

the western Mediterranean Sea. This margin provides an ideal site for our study – it has been surveyed with high resolution multibeam echosounders during various research cruises (Amblas et al., 2006), its overall stratigraphy and structure are spatially uniform and well constrained (Alonso et al., 1990; Farrán and Maldonado, 1990; Field and Gardner, 1990), and the margin is presently incised by numerous submarine canyons and canyon-channel systems (Canals et al., 2000).

We focus our study on submarine canyons in passive margins for two reasons. First, submarine canyons play an important role in margin development globally and act as sinks and conduits for sediment particles and associated nutrients, organic carbon and pollutants (Shepard, 1981; Normark and Carlson, 2003; Puig et al., 2004; Allen and Durrieu de Madron, 2009; Harris and Whiteway, 2011; Sànchez-Vidal et al., 2012; Canals et al., 2013). In spite of their relevance and widespread distribution, the genesis and evolution of submarine canyons continues to be debated (Bertoni and Cartwright, 2005; Pratson et al., 2009). We attribute this to three reasons: (i) complexity and diversity of canyon topographies from different continental margins (Harris and Whiteway, 2011); (ii) difficulties faced by geoscientists in observing contemporary sediment transport and canyon formation processes directly on site (see review by Puig et al., 2014); and (iii) the fact that present-day processes may provide limited understanding of canyon evolution because many submarine canyons could be relict features that may only bypass sediment from the continental shelf to the deep basins (Emery and Uchupi, 1972; Vail et al., 1977; Burger et al., 2001). Space-for-time substitution can therefore be an important tool to derive information on the changing nature of canyon formation processes and associated morphology with time, which provides a framework for interpreting the relative age of erosion morphologies on continental

slopes. Secondly, passive margins provide less complicated geological settings than active margins, which simplifies our investigation of the evolution of submarine canyon–channel systems. Passive margins also comprise two-thirds of the world's continental margins and host 40% of global submarine canyons (Harris and Whiteway, 2011).

2. Regional setting

The Ebro Margin is a 22,000 km^2, NE–SW trending passive margin formed on the western shoulder of the Valencia Trough between the Iberian Peninsula and the Balearic Promontory (Bertoni and Cartwright, 2005; Amblas et al., 2006; Fig. 1). It comprises a progradational shelf–slope system that has been active during the Plio-Pleistocene and that is driven by the influx of terrigenous sediment from the Ebro River (Field and Gardner, 1990; Fig. 1). The Ebro Margin consists of stacked shelf-margin deltaic and slope depositional units, which reach a thickness of 2.5 km; these units are separated by disconformities and lie above the erosion surface formed during the Messinian Salinity Crisis (Alonso et al., 1990; Farrán and Maldonado, 1990; Kertznus and Kneller, 2009). The growth patterns of the Ebro Margin have been controlled by glacio-eustatic sea-level oscillations, subsidence, and changes in sediment type and discharge from the Ebro River, which were up to three times higher during Quaternary lowstands (Farrán and Maldonado, 1990; Canals et al., 2000). During sea-level highstands, such as at present, lower energy hemipelagic sedimentation prevail over the entire margin (Alonso et al., 1990). Currently, most of the sediment supplied by the Ebro River is trapped by dams or in the delta (Palanques et al., 1990).

The Ebro continental shelf consists of a 70 km wide, gently sloping (up to 0.5°), smooth seabed that is disrupted in the south by the small volcanic archipelago of Columbretes Islets (Fig. 1B). The shelf break is almost parallel to the coast and occurs at depths ranging between 100 and 130 m. The outer continental shelf is sand-dominated, whereas muddy deltaic deposits cover the inner continental shelf (Díaz et al., 1996). The continental slope is only 10 km wide and has a slope gradient of up to 10°. Numerous canyons are incised in the continental slope and outer continental shelf. Some of these canyons evolve into well-developed turbiditic channel–levée complexes at their lower courses, forming the Ebro turbidite system (Alonso and Maldonado, 1990; Field and Gardner, 1990; Canals et al., 2000; Casas et al., 2003; Amblas et al., 2006). Recurrent slope instability failures have interrupted the development of a number of these canyon–channel systems (e.g. Lastras et al., 2002).

The Ebro continental shelf is a micro-tidal, low energy oceanographic setting. Mesoscale circulation is dominated by the Northern Current, an along-slope, southward flowing, cyclonic steady geostrophic current that flows along the middle to outer continental shelves and slopes (Font et al., 1990). Sediment transport on the Ebro continental shelf is mainly directed towards SSW and the mean along-shelf sediment flux greatly dominates over the mean seaward cross-shelf flux, being driven by storm events, strong wind-induced currents and the occurrence of near-inertial internal waves at the base of the thermocline (Cacchione et al., 1990; Puig et al., 2001; Palanques et al., 2002).

Our study area is located in the southern limit of the Ebro Margin, where the shelf break turns landwards to the south of Columbretes Islets (Fig. 1B). There, the continental slope changes its

orientation from NE–SW to E–W and has a slope gradient that ranges between 5.3° and 6.3°. It is incised by numerous, closely spaced submarine canyons and an NW–SE oriented canyon–channel system, which extends from the outer continental shelf to a depth of ~1400 m (Fig. 2). This canyon–channel system is known by the name of South (or Great) Columbretes Canyon (Canals et al., 2012). Similar canyon-channel systems, such as North (or Small) Columbretes Canyon (Fig. 2) and Orpesa Canyon (Amblas et al., 2006), are located north-east of the study area. For ease of simplicity, South and North are utilised to refer to these two canyons from here onwards.

3. Materials and methods

3.1 Bathymetric and backscatter data

We base our study on data collected during six multibeam echosounder surveys on board *BIO Hespérides, RV L'Atalante* and *BO García del Cid*. The first dataset, acquired during "BIG'95" cruise in 1995 with a Simrad EM-12S system, covers the eastern part of the study area and the entire canyon–channel system. The second dataset was collected during "CALMAR" cruise in 1997 with a Simrad EM-12 system and covers the upper continental slope of the Ebro Margin. The third dataset was acquired from the outer continental shelf during "MATER-2" cruise in 1999 using a Simrad EM-1002S system. Bathymetry and backscatter grids of 50 m cell size were generated from these datasets. The fourth dataset was collected during "EUROLEON" cruise in 2007 using a Simrad EM-120 system and covers most of the south Ebro Margin. The fifth and sixth bathymetric datasets were acquired with shallow depth Seabeam Elac 1050D 180 kHz

multibeam echo-sounder during cruises "CASCADES" in 2009 and "COSTEM" in 2010, and covered the outer shelf and upper slope region of the south Ebro Margin. These data sets were processed to generate bathymetry and backscatter grids of 20 m cell size.

3.2 Nomenclature of seafloor morphology and morphometric measurements

In this paper we differentiate between three types of seafloor erosional morphologies: gullies, canyons and canyon–channel systems. Gullies are short (<2 km in thalweg length), elongate depressions with little relief (<10 m), whereas canyons are longer and deeper valleys (Field et al., 1999; Harris and Whiteway, 2011). Gullies are restricted to the continental slope whereas canyons may also extend into the continental shelf. A canyon–channel system comprises a canyon and its downslope extension across the lower continental slope and continental rise in the form of a channel (Clark and Pickering, 1996). We collectively refer to these three types of seafloor morphologies as valleys.

To test our hypothesis that space can be substituted for time to reconstruct the evolution of a submarine canyon–channel system, we used valley thalweg length as an ergodic indicator of landform development. We organised the six easternmost valleys into a sequence of increasing valley thalweg length and labelled these valleys as 'feature' 1–6 (Figs. 3 and 4). For each feature we mapped the valleys and their tributaries as a network of lineaments and extracted a number of morphometric parameters from the bathymetric datasets (Fig. 5; Table 1). We focused our study on the six easternmost valleys because they exhibit evidence of relatively recent erosional activity. This evidence comprises sharply defined morphologies and high backscatter along the

valley beds. These characteristics contrast with those of valleys located to the west (e.g. features X–Z in Fig. 3). These valleys display smoother morphologies and low backscatter along the valley axes and their tributaries.

3.3 Hydrodynamic conditions, sediment fluxes and sediment accumulation rates

Field measurements of contemporary hydrodynamic conditions and sediment fluxes were carried out with near-bottom instrumented moorings deployed in the heads of two of the studied canyons (Fig. 2). Mooring 1 (M1) was deployed at 300 m depth in the South Columbretes Canyon (feature 6; 39º41.92' N; 0º39.50' E) from October 2008 to January 2009. Mooring 2 (M2) was deployed at a depth of 500 m in one of the branches of feature 5 (39º38.42’ N; 0º30.91’ E) during three consecutive periods between May 2010 to June 2011. M1 was equipped with an Aanderaa RCM-9 current metre with temperature, pressure, conductivity and turbidity sensors placed at 5 m above the bottom (mab). M2 was also equipped with an Aanderaa RCM-9 current metre and included a sequential sediment trap Technicap PPS3 with 12 collecting cups placed at 30 mab. Time series for four months and one year were collected from M1 and M2, respectively. The current metres’ sampling interval was set to 30 minutes for both moorings. The sediment trap collection intervals in M2 varied between 9 and 12 days, depending on the deployment period. Turbidity data recorded by current metre sensors were converted from the formazin turbidity units (*FTU*) into suspended sediment concentration (*SSC*) following the general equation obtained by Guillén et al. (2000) using in situ measurements from the western Mediterranean:

$$SSC\ (\text{mg l}^{-1}) = 1.74(FTU - FTU_{\text{min}}) \quad (1)$$

where FTU_{min} is the minimum turbidity recorded by the sensor during a given deployment period. When particulate matter remains suspended in the water column, we can make the assumption that the sediment particles move with the velocity of the water within which they are suspended (Wright, 1995). Therefore, the instantaneous suspended sediment flux can be obtained by multiplying the instantaneous values of the horizontal current velocity components and *SSC*. In order to obtain the across- and along-canyon sediment fluxes, a clockwise rotation of the coordinates system of 5º in M1 and 25º in M2 was performed using the canyon axis orientations obtained from the multibeam bathymetry data as reference. Based on these rotations, time-integrated cumulative across- and along-canyon sediment transport were calculated.

In the laboratory, M2 sediment trap samples were treated following some of the procedures described by Heussner et al. (1990). Once the particles were settled down in a solution, the supernatant was removed by pipette and stored apart. The living organisms that actively entered the trap were removed from the samples. In order to extract all the sea water, the sieved material was washed with Mili-Q water and centrifuged three times. The sediment trap samples were subsequently frozen and lyophilised. Downward particles fluxes were computed using the total mass weight (in g, extracted from the dry weight of each sample), the trap collecting area (in m^2) and the sampling interval (in days).

In addition, a subsurface sediment core was taken at the site of M2 using a KC multicorer with six collecting tubes. Immediately after retrieval, one of the tubes was sub-sampled in 1 cm slices

and stored in sealed plastic bags at 4ºC. The sediment accumulation rate from this core was estimated from ^{210}Pb concentration profiles. ^{210}Pb activities were determined through the measurement of its daughter nuclide ^{210}Po, which is assumed to be in radioactive equilibrium with ^{210}Pb in the sediment samples, using a method modified after Nittrouer et al. (1979). Analyses of the sediment samples were performed by total digestion of 200–300 mg using the methodology described by Sanchez-Cabeza et al. (1998). ^{210}Po was added to each sample before digestion, as an internal tracer, and Polonium isotopes were counted with an alpha spectrometer equipped with low-background silicon surface barrier (SSB) detectors (EG&G Ortec).

4. Results

4.1 Contemporary current and sediment fluxes within canyon heads

Time series of current speed, *SSC*, cumulative transport (along and across-valley) and sediment flux in feature 6 for the period October 2008 to January 2009 and in feature 5 for the period May 2010 to June 2011 are shown in Fig. 6. In feature 6, the current speeds reached values of 15–20 cm s^{-1} (Fig. 6A), and the *SSC* record was considerably low, with values of 0.5 mg l^{-1} for all the time series (Fig. 6B). Cumulative transport across-valley was in an SSE direction and was slightly lower than the along-valley transport, which reached values of 0.03 T m^{-2} (Fig. 6C). In feature 5, the current speed time series maintained relatively low values from May 2010 to February 2011, and increased slightly from February to June 2011, reaching values of > 20 cm s^{-1} (Fig. 6D). The *SSC* record was again considerably low during all the time period, mostly below 0.5 mg l^{-1} (Fig. 6E). Cumulative transport across-valley was also in an SSE direction and almost

negligible, while cumulative flux along-valley was downslope, reaching values of 0.02 T m^{-2} (Fig. 6F). The sediment transport along feature 5 is much lower than that in feature 6. Low values (<2 g m^{-2} d^{-1}) were recorded for total mass fluxes in feature 5, accounting for an annual flux of 640 g m^{-2} y^{-1} (Fig. 6G). In October 2010, an increase in current speed, caused by an energetic (Hs >4.5 m, Tp >10 s) northern storm affecting the study area, increased the sediment flux to 7.2 g m^{-2} d^{-1}. The annual downward particle flux for the time period 2010–2011 accounted for 640 g m^{-2} y^{-1}. No comparison can be made with the valley in feature 6 because no downward particle flux data were recorded. A ^{210}Pb-derived sediment accumulation rate of 900 g m^{-2} y^{-1} and a sedimentation rate equivalent to 0.137 cm y^{-1} were calculated for feature 5 at site M2.

4.2 Valley morphologies

Fig. 7 presents maps of the different valleys identified in the study area. An individual gully (feature 1) is the smallest erosional morphology identifiable. Its head is defined by a steep, arcuate scarp located on the continental slope 1.3 km down from the continental shelf break at a depth of ~380 m (Figs. 3 and 7). Gullies of equivalent size and form are observed on the continental slope to the east of the study area, at a similar water depth and distance from the shelf break. In features 2 to 5, the valley develops from a gully into a canyon with gullies and smaller canyons as tributaries (Figs. 3 and 7). The thalwegs of the largest features 4 and 5 are located at a distance of 3 km from each other; this is the same distance that separates the three valleys of comparable thalweg length located to the west of the study area (labelled X–Z in Fig. 3). The upslope boundaries of features 3 and 4 are contiguous, whilst the termini of features 2 and 3

connect with those of features 4 and 5, respectively (Fig. 3). An abandoned canyon can be identified to the west of feature 5 (Fig. 8A).

In features 2–5, the predominant types of valley head and wall erosional features comprise (i) first to fifth-order gully networks with sharp interfluves, and (ii) smooth and well-defined scars located at, or in the vicinity of, the gully heads and along valley walls (Figs. 3 and 8A). The gully networks are concentrated in the upper valley section (< 800 m depth). The steepest areas within all the valleys are located at the heads of the tributary gullies, scar headwalls, and along the valley walls. Gullies join the main valley axis where the valley depth is largest. The valley axes are characterised by an absence of failure deposits. A series of asymmetric scours are observed close to the valley terminus of feature 5 (Figs. 7 and 8C). The valley courses in features 5 and 6 are characterised by hanging gullies and multiple terraces that are up to 80 m high (Fig. 8A,D). The valley heads of features 4–6 breach the continental shelf (Figs. 3, 4 and 7). The head of the valley in feature 5 is linked by 100 m wide and 4 m deep elongate depressions to a sand body (Fig. 8B). This sand body is intersected by the head of feature 6, which comprises an extensive canyon–channel system (Fig. 4A and 7). This valley features gullies and failure scars in the upper reaches, whereas it becomes more sinuous downslope, with a hanging ox-bow and levées up to 50 m high (Fig. 8D).

4.3 Valley morphometrics

For all features in our study area, axial gradient and valley depth decrease away from the valley head (Fig. 9A–C). Valley downslope profiles are concave and lack knickpoints (Fig. 9A). The

profile of feature X, in comparison, is convex–concave (Fig. 9D). Gully downslope profiles are steeper (mean gradient of 15°) and less concave than those of the canyons. With increasing thalweg length, the valley cross-sectional shape changes from V- to U-shaped.

We observe a progressive increase in width, valley depth, width:depth ratio, area, volume, and number and thalweg length of tributary valleys with increasing thalweg length from features 1 to 6 (Fig. 10A,B,C,G). The most significant changes in valley dimensions are recorded in valley thalweg length. The majority of across-slope elongation takes place downslope of the valley (Figs. 7 and 10E). Valley axial slope gradient decreases exponentially with thalweg length (Fig. 10D).

Breaching of the shelf break (between features 3 and 4) and connection of the valley head with the outer shelf sand body (features 5 and 6) are associated with significant changes in valley morphology (Fig. 7). Shelf-breaching results in: (i) most of the material being eroded from the upper valley reaches, which is in contrast to what we observe in features 1–3, where the majority of the material is eroded from the lower valley reaches (Fig. 10F); and (ii) temporary reduction in downslope valley elongation and increase in drainage density (Fig. 10D,F). Connection of the valley head with the sand body, on the other hand, results in: (i) a rapid increase in valley area, volume, width, width:depth ratio, depth of the main valley axis, and the number and thalweg length of tributary valleys (between features 4 and 5; Fig. 10A,B,C,G); and (ii) a rapid downslope elongation of the valley in correspondence with unchanging valley width and depth (between features 5 and 6) (Fig. 10A,E).

Prior to the formation of the canyon–channel system (features 1–5), the following relationships are observed: (i) linear length correlates positively with valley width according to a linear equation (Fig. 11C); (ii) valley profile concavity tends to increase asymptotically with thalweg length (Fig. 11D); and (iii) valley thalweg length increases asymptotically with valley area according to a positive power law with an exponent of 0.46 (Fig. 11A). The above morphometric relationships do not apply to feature 6 because of an abrupt increase in thalweg length (Fig. 11A,C) and concavity (Fig. 11D).

With increasing thalweg length, the following changes in canyon network parameters are also observed: (i) bifurcation ratios decrease progressively to a value of 4.2; (ii) drainage density decreases (Fig. 10D); and (iii) slope gradient decreases and thalweg length of valleys and tributaries increases with increasing stream order (Fig. 11B).

5. Discussion

5.1 Evolution of the south Ebro Margin submarine canyon–channel system

5.1.1 Inferred morphological evolution of the canyon–channel system

Morphologic evidence from the south Ebro Margin leads us to propose that valley evolution starts as a first-order gully eroded on the continental slope that develops into a shelf-breaching dendritic canyon and, finally, into a canyon–channel system extending into the lower continental slope and rise (Fig. 7). The majority of canyon growth involves downslope extension of the

valley (Fig. 10E). Initially, most of the material is removed from the lower reaches of the valley (Fig. 10F). These initial stages are also dominated by incision, and the rates of changes in valley depth are faster than those in valley width. Upslope elongation also occurs, to a lesser extent, by repeated retrogressive slope failure of the valley head. Valley deepening creates steep walls that fail due to oversteepening and loss of support at their base, as indicated by the numerous scars identified in features 2–5. Flank failures are responsible for widening the valley and introducing material into the valley thalweg. Where the valley has been incised the deepest, the scars of these flank failures develop into long and steep tributary gullies. Valley elongation and widening is also likely responsible for piracy of adjacent sediment drainage. The contiguity of features 2–5 and the abandoned canyon leads us to propose that the development of individual valleys has been halted or slowed down by the faster growth of adjacent, larger valleys, which would have captured sediment drainage and focused it along their main conduits.

We propose that erosion of the valleys is driven by gravity flows triggered in the upper slope. Evidences for this inference include: (i) the decrease of valley depth with distance downslope (Fig. 9B,C) and the concentration of gullies upslope (Fig. 7), which are indicative of an erosive process with a source in the upper valley reaches; (ii) the concave shape of the thalweg downslope profile (Fig. 9A), which is indicative of loss of flow competence from valley head to mouth as it erodes and transports material (Gerber et al., 2009; Covault et al., 2011); (iii) the absence of failure deposits on the valley floor and the high backscatter values along the valley beds, which indicate that the deposits were likely removed by gravity flows (Figs. 3, 4 and 8A,D); and (iv) the occurrence of terraces in features 5 and 6, which we interpret as evidence of multiple events of axial incision (Fig. 8A,D; Baztan et al., 2005). The initiation of

equidimensional gullies on the continental slope at a similar distance from the shelf-break (feature 1) may be explained by two mechanisms. The first is gully incision by unconfined, shelf-originating, downslope-accelerating gravity flows (Micallef and Mountjoy, 2011). These high-density, gravity-driven flows exert tractive forces on the seafloor that increase with distance downslope from the shelf break. When the basal stress is high enough to overcome the shear resistance of the seabed material, the seafloor is eroded and a small irregularity is formed. Channelisation of the unconfined gravity flow into these proto-gullies may occur by either topographic roughness or flow instability (Lastras et al., 2011; Micallef and Mountjoy, 2011). A second mechanism is spring sapping, which involves the discharge of groundwater or another type of fluid from the face of the continental slope at a specific depth or stratigraphic level (Orange et al., 1994; Pratson et al., 2009). Apart from explaining the occurrence of numerous gullies at a similar water depth and distance from the shelf break, this process would also account for the smooth, undisturbed seafloor observed upslope of the gully heads. The lack of direct evidence of fluid sapping may be attributed to seafloor erosion and valley enlargement for features 2–6. The exertion of force from seepage and gravity would cause the sediments on the slope to fail, which would explain the initiation and continued failure at the gully's head and its upslope growth. For gully downslope elongation to occur, however, erosion by gravity flows is still required.

The advanced stages of valley development are characterised by a sharp increase in valley growth. First, the valley head breaches the continental shelf break, allowing it to capture large volumes of sediment directly from the shelf, and shifting the locus of erosion to the upper reaches of the valley (features 4–5). This results in pronounced valley deepening, lateral

widening and increase in the number of tributary valleys in the upper reaches (Fig. 10A,B,G; feature 5). Secondly, the valley head directly connects with the outer shelf sand body (feature 6). This sand body has been interpreted as outer shelf palaeo-delta deposits, with an estimated age of about 11,100 yrs BP, which mark where palaeo-rivers deposited sediment in the outermost shelf and upper slope of the Ebro Margin during sea-level lowstands (Díaz et al., 1990; Farrán and Maldonado, 1990; Lo Iacono et al., 2010; Fig. 8B). Connection with the palaeo-delta could have significantly increased the flow of sediment into the valley head, leading to the formation of the channel at the base of slope (feature 6). The initiation of the channel is marked by the formation of a series of scours at the mouth of the canyon (feature 5), which we interpret as cyclic steps formed by repeated gravity flows evolving from confined to unconfined conditions (Parker and Izumi, 2000). The scours eventually coalesce into a more continuous channel thalweg (feature 6). At this stage, valley development entails extensive valley elongation, with limited widening or deepening, into the gently sloping lower continental slope and continental rise. In the lower reaches of the channel, morphologies associated with channel development and migration develop. These include a sinuous valley course, abandoned channel branches, and hanging ox-bow and channel-levée systems (Canals et al., 2000) (Fig. 8D).

5.1.2 Source of gravity flows

Processes that trigger the gravity flows that are thought to have driven valley evolution in the south Ebro Margin may include seismic activity associated with regional volcanic and tectonic processes, oversteepening of the prograding upper slope by rapid sedimentation, and cyclic wave loading (Canals et al., 2000). Although seismic activity of small magnitude is present in the Ebro

Margin (Grünthal et al., 1999), this cannot explain the regularity of canyon occurrence along the entire Ebro Margin. We suggest that the most likely source of gravity flows is oversteepening and failure of the outermost shelf and upper slope due to rapid sedimentation by palaeo-rivers during sea-level lowstands (Farrán and Maldonado, 1990; Piper and Normark, 2009). The heightened sediment supply and depositional oversteepening associated with the palaeo-river delta would have had the potential to frequently trigger gravity flows that would have incised the valleys in our study area. The direct association between the increase in valley development and the connection of the valley with the palaeo-river in feature 5 provides further support to our inference (Figs. 4A and 8B). A second possible mechanism triggering gravity flows during sea-level lowstands is the action of waves during storms (Parsons et al., 2006). A recent review of contemporary sediment transport processes in submarine canyons, which includes observations in canyons incised on tectonically active margins or nearby major rivers that may be analogues for sedimentary processes during low-stands of sea level, highlights the combined effect of storms and river floods (concurrent or delayed in time) as an important component for shelf-to-canyon sediment-gravity flow transport in many continental margins (Puig et al., 2014). However, wave action has also been shown to be an important process generating sediment gravity flows at present sea-level in submarine canyons whose heads are located at shelf-break depths and far away from the shore (e.g. Puig et al., 2004).

5.1.3 Timing of valley activity

The above considerations suggest that valley development in the south Ebro Margin was likely more pronounced during sea-level lowstands, when the shoreline would have been close to, or

was intersected by, the heads of the more developed canyons at the present shelf break (Figs 1 and 2; Lambeck and Bard, 2000). The mid-Pleistocene to Holocene period is associated with rapid high-amplitude sea-level fluctuations and increased sedimentation along the Ebro Margin (Nelson, 1990; Kertznus and Kneller, 2009). Due to their contrasting bathymetric and backscatter signatures, we infer that the valleys to the west of the study area (e.g. features X–Z in Fig. 3) have formed by erosion episodes that pre-date those in the study area; since then, valleys X–Z have undergone subsequent infilling by hemipelagic background sedimentation and margin progradation, as indicated by the convex–-concave downslope profile of valley X (Fig. 9D; Gerber et al., 2009). The valleys in our study area, on the other hand, have been active more recently, most likely during or shortly after the Last Glacial Maximum sea-level lowstand. This difference in the timing of valley activity may be explained by the eastward shift of the palaeo-river delta during the same or earlier sea-level lowstands, as has been documented by Farrán and Maldonado (1990). Multiple terraces in features 5 and 6 in our study area, on the other hand, evidence numerous periods of reactivation during the same or different sea-level lowstands (Baztan et al., 2005; Antrobreh and Krastel, 2006). The palaeo-river is likely to have been an extension of the Mijares River, which is the second largest terrestrial fluvial system draining into the Ebro Margin and which is located closer to the study area in comparison to the Ebro River (Farrán and Maldonado, 1990; Field and Gardner, 1990; Urgeles et al., 2011).

Field observations from instrumented moorings in features 5 and 6 between 2008 and 2011 indicate that contemporary sediment transport is relatively small, current velocities are weak and SSC is low (Fig. 6). The major storm event occurring in mid-October 2010 during the deployment in feature 5, which had a recurrence period of more than 4 years (Puertos del Estado,

2013), did not trigger a sediment gravity flow and only increased the downward particle fluxes within the canyon as a consequence of off-shelf suspended sediment advection (Fig. 6). Furthermore, the mean annual downward particle fluxes measured by sediment traps are similar to the mean sediment accumulation rates measured by ^{210}Pb in the same site (~ 640 vs 900 g m^{-2} y), suggesting a similar sediment transport regime in feature 5 during at least the last century.

From all of this we can infer that: (i) submarine valley activity across the southern Ebro Margin has been pulsating and correlated with sea-level lowstands; this contrasts with the larger and wider submarine canyons incising the north Catalan margin and located 260 km to the northeast (e.g. Blanes, La Fonera, Cap de Creus canyons), which currently manifest a high degree of activity in terms of water and sediment transport (e.g. Canals et al., 2006; Puig et al., 2008; Zúñiga et al., 2009; Ribó et al., 2011); and (ii) valley morphology in this passive, progradational margin can be maintained over the course of more than one fall and rise in sea-level, in agreement with the conclusions by Amblas et al. (2012).

5.2 Validity of the space-for-time substitution model

The inferred model for the morphological evolution of submarine canyons and channels in the south Ebro Margin shows many parallels with established models in the literature.

In terms of submarine canyon evolution, two models have been widely cited in the literature:- the upslope and downslope erosion models. Observations of canyons on the Atlantic margin of North America have led many scientists to propose a model involving the upslope development

of a canyon from the continued retrogressive failure of a landslide complex initiated on the continental slope (Shepard and Dill, 1966; Normark and Piper, 1968; Shepard and Buffington, 1968; Shepard, 1981; McGregor et al., 1982; Twichell and Roberts, 1982; Farre et al., 1983; Posamentier et al., 1988; Normark and Piper, 1991). More recent studies, based on the investigation of old buried canyon courses and integrating the ideas of Daly (1936), propose the downslope erosion model (Pratson et al., 1994; Pratson and Coakley, 1996). In these works, the authors invoke the need for both gravity flow erosion and retrogressive slope failure for submarine canyon formation. Downslope sediment flow, induced by depositional oversteepening and localised failure of the upper continental slope, is considered the major driver of canyon initiation, which takes place in the upper continental slope through erosion of pre-canyon gullies. These gullies act as topographic constraints from which submarine canyons and channels develop. As these gullies grow into canyons, they widen through localised slope failure of the oversteepened walls caused by destabilisation by sediment flow incision. The upslope advance of the canyon is driven by retrogressive failure of the canyon head by sediment flow erosion. Valley piracy plays an important role in establishing a main sediment drainage conduit in the initial stages of the downslope erosion model. This model has been shown to explain canyon evolution in many margins around the world, e.g. Angolan (Gee et al., 2007); South African (Green et al., 2007); Equatorial Guinean (Jobe et al., 2011); Chilean (Laursen and Normark, 2002); Californian (Paull et al., 2003, 2005, 2013); Gulf of Lions (Sultan et al., 2007); and others (e.g., Normark and Carlson, 2003; Pratson et al., 2009)). Our inferred valley evolution model for the south Ebro Margin best corresponds to the downslope erosion model.

Shelf breaching is an important factor in our model. The significance of shelf breaching was first demonstrated by Farre et al. (1983), who showed how connection to shelf-sourced sediment contributes to the development from "youthful" to "mature" canyons. Valley evolution in our study area appears to be most active when sediment influx to the slope is greatest, which coincides with sea-level lowstands. Features 5 and 6, for example, have likely gone through several phases of erosion and deposition as sea-level changed and shelf-edge depocentres shifted. These patterns have been widely reported in the literature (Daly, 1936; Felix and Gorsline, 1971; Twichell et al., 1977; Vail et al., 1977; Stanley et al., 1984; Posamentier et al., 1988; Bertoni and Cartwright, 2005; Pratson et al., 2009). Submarine channel inception via a series of scours has been documented in many recent studies (Pirmez and Imran, 2003; Fildani and Normark, 2004; Fildani et al., 2006; Normark et al., 2009; Kostic, 2011; Covault et al., 2012; Fildani et al., 2013), as has the development of channel–levée systems in the channel marginal regions (Fildani et al., 2006, 2013; Armitage et al., 2012).

Because our inferred model and observations agree with evolution models and case studies reported widely in the literature, we can conclude that our hypothesis is validated and that time can be substituted by space when reconstructing the evolution of submarine canyon and channel systems in the south Ebro Margin. This means that valleys ordered in a sequence of increasing thalweg length represent an evolutionary pathway of stages of increased landform development. Can the space-for-time substitution also be used to infer the age of the submarine valleys? We cannot establish the age of the valleys from our data set, and this would be a difficult endeavour anyhow because submarine valleys are erosive features that cut the sediments accumulated during the onset of their formation (Pratson et al., 2009). There also exists the possibility that the

valley piracy may have slowed down or halted the development of valleys 2–4. Inferring landform age directly from morphology is therefore difficult.

There is also the possibility that morphological differences observed in the valleys in our study area are a result of different seafloor processes or conditions rather than extent of landform development or age. We do not think that this is the case. Our study area is relatively small (~500 km^2) and the continental slope is characterised by quasi-uniform slope gradient, structure, substrate and oceanographic conditions (Farrán and Maldonado, 1990; Field and Gardner, 1990; Font et al., 1990; Amblas et al., 2006, 2011, 2012; Urgeles et al., 2011). The material being eroded is predominantly Plio-Quaternary shelf-margin deltaic and slope depositional units, whilst the control of extensional and thrust faults on the seafloor is more important further south. Influence from other rivers, such as the Ebro, is unlikely because its mouth was located at least 15 km from the head of feature 6 during the last sea level lowstand (Farrán and Maldonado, 1990), and because shelf edge depocentres across the Ebro Margin only fed one canyon at a time (Alonso et al., 1990).

5.3 *New insights into submarine canyon-channel system evolution in a passive progradational margin*

Since the space-for-time substitution model can be applied to the south Ebro Margin, we use some of the morphometric results derived in Section 4.3 to identify patterns in the morphological evolution of submarine canyons. These patterns include:

(i) Valley planform shape is geometrically similar at consecutive stages of evolution, as indicated by the isotropic scaling of linear length with width and compliance with Hack's Law with an exponent <0.5 (Fig. 11A,C; Hack, 1957). This is similar to what has been observed in terrestrial river drainage basins (Montgomery and Dietrich, 1992; Rigon et al., 1996; Dade, 2001).

(ii) Canyon longitudinal profiles evolve towards equilibrium between canyon form and imposed water and sediment load, with no net erosion or deposition taking place. This is demonstrated by the exponential decay of thalweg slope gradient and asymptotic growth of profile concavity with increasing thalweg length (Figs. 9A and 10D). This pattern has been reported in submarine channels (Pirmez et al., 2000; Kneller, 2003).

(iii) Canyon draining efficiency increases, and energy expenditure is minimised, with evolution, as implied by the decrease in drainage density and bifurcation ratio with increasing thalweg length (Fig. 10D), in spite of increasing water and sediment loads. This has been documented in terrestrial drainage basins (Rinaldo et al., 1992).

The variations of valley slope gradient and thalweg length with stream order (Fig. 11B) also show that submarine canyons share additional morphologic similarities with terrestrial drainage basins.

The following three relationships – isotropic scaling of linear length with width, compliance with Hack's Law, and asymptotic growth of profile concavity with thalweg length – no longer apply when feature 6 is included in the plots (Fig. 11A,C,D). We interpret this as clear evidence of a significant geomorphological system change due to an extrinsic disturbance. This disturbance is

of the ramp type (Brunsden and Thornes, 1979), involving a sustained increase in sediment flow into the canyon related to the direct connection of the palaeo-river with the canyon head. The response to this disturbance is a considerable change in the valley formation dynamics, entailing a shift from a process domain characterised by deepening and lateral widening of the canyon's upper reaches, to one dominated by extensive downslope elongation and the formation of a channel and associated deep-water deposits.

Our study also provides interesting insights into the early stages of canyon development. First, canyon elongation is generally higher downslope, which contrasts with the predominant headward development of submarine canyons reported in numerous models (e.g. Pratson et al., 1994, 2009). Second, the canyon goes through an early stage of rapid incision, where the rate of change of depth is much higher than that of the width, and where wall erosion is minimal. This is very similar to the process of "erosion narrowing" reported in terrestrial rivers (Cantelli et al., 2004). Third, the increase of the valley to depth ratio from 7.5 to 20.3 (Fig. 10B) indicates that the valley widens more than it deepens with maturity, suggesting that the influence of flank slope failures increases as the valley develops.

One final consideration relates to the regular spacing observed between features 4, 5, X, Y and Z. We have two explanations for this. The first is that regular spacing emerges over time due to competition for drainage area, as proposed for terrestrial landscapes (Perron et al., 2009). As irregularly spaced incipient valleys grow, competition for drainage area leads some valleys to capture more area. This halts the growth of neighbouring valleys that are either too small or closely spaced, resulting in the topography approaching a deterministic equilibrium where valley

spacing is approximately uniform (Perron et al., 2008). A second cause of regular spacing may be spring sapping interacting with slope failure processes (Orange et al., 1994). The creation of high head gradients at canyons leads to a reduction in the head gradient in the surrounding seafloor, which results in the fastest growing valleys capturing flow of smaller neighbouring valleys. We therefore propose that the occurrence and extent of regular spacing between valleys across the south Ebro Margin is determined by valley piracy.

5.4 Applicability of our results to other margins

The conclusions we have derived so far are likely applicable to the majority of the Ebro Margin because it is characterised by a similar sedimentary and structural setting to that of our study area (Canals et al., 2000). The canyon–channel systems located in this region share similar dimensions and morphologies to those in our study area, including regular spacing and downslope elongation. They locally differ, however, in having been connected to different palaeo-rivers and in their interaction with large-scale slope failures.

The described patterns in the morphological evolution of submarine canyons may be applicable to other passive margins around the world. The Atlantic passive margin of the USA is comparable to the Ebro Margin; canyons are initiated by sediment flows triggered along the shelf edge and upper slope, and their development was driven by lateral shifts of shelf-edge delta depocentres (Farrán and Maldonado, 1990; Pratson et al., 1994). Examination of published data from the USA mid-Atlantic margin, for instance, reveals that the canyons are regularly spaced and those do not incise the shelf share a similar canyon head depth but different canyon terminus

depths, indicating that downslope elongation was prevalent (Pratson et al., 1994; Mitchell, 2004; Brothers et al., 2013a,b; Vachtman et al., 2013; Obelcz et al., in press). The above similarities also apply to the Ligurian, north-west Black Sea and Equatorial Guinea margins (Popescu et al., 2004; Jobe et al., 2011; Migeon et al., 2011).

The applicability of the space-for-time-substitution concept is potentially wide. Apart from the USA Atlantic margin, where Twichell and Roberts (1982) and Farre et al. (1983) used the concept to reconstruct canyon evolution by retrogressive failure, space-for-time-substitution appears to be valid in a number of settings recently documented in the literature. High resolution seafloor data sets from offshore La Réunion Island, which comprises a shield volcanic island where a direct connection between terrestrial rivers and submarine canyon exists, show that successive stages of canyon formation can be interpreted from variations in canyon thalweg length and morphologies (Babbonneau et al., 2013). Seafloor data from the Argentine passive continental margin have been interpreted to show how the longer, more developed canyons in the north are likely more long-lived features than the shorter canyons in the south, where canyon formation is more incipient (Lastras et al., 2011).

6. Conclusions

In this study we analysed multibeam echosounder data and in situ measurements from the south Ebro Margin to test whether the concept of space-for-time substitution can be used to reconstruct the evolution of a submarine canyon–channel system in a passive progradational margin. By organising selected submarine valleys in a sequence of increasing valley thalweg length and

analysing their morphology and morphometry, we were able to propose a morphological model of submarine valley evolution. This model entails the development of a first-order gully eroded on the continental slope into a shelf-breaching dendritic canyon and, finally, into a canyon–channel system extending into the lower continental slope and rise. Two processes are responsible for valley erosion – gravity flows, likely sourced by failure of the outermost shelf and wave loading during sea-level lowstands, and flank slope failures. The initial stages are dominated by incision and downslope elongation. As the valley develops, shelf breaching and connection with a palaeo-river result in a sharp increase in valley growth in the upper reaches and in the formation of a long, sinuous channel. Since our model shows many parallels with established models in the literature, we conclude that time can be substituted by space when reconstructing the evolution of submarine canyon and channel systems in the south Ebro Margin. This means that valleys ordered in a sequence according to their thalweg length represent evolutionary pathway of stages of increased landform development.

Morphometric results derived from the application of space-for-time substitution model in the south Ebro Margin allowed us to gain new insights into the morphological evolution of submarine canyons in a passive progradational margin. These include the following: (i) canyon planform shape is geometrically similar at consecutive stages of evolution; (ii) canyon longitudinal profiles evolve towards equilibrium between canyon form and imposed water and sediment load; (iii) canyon draining efficiency increases and energy expenditure is minimised with evolution; (iv) canyon elongation is generally higher downslope; (v) canyons go through an early stage of rapid incision similar to the process of "erosion narrowing" reported in terrestrial rivers; and (vi) the influence of flank slope failures increases as the canyon develops.

We demonstrate that the conclusions of our study are not limited to submarine valleys in the south Ebro Margin but they are applicable to other margins around the world.

Acknowledgements

This research was supported by Marie Curie Intra-European Fellowship PIEF-GA-2009-252702, Marie Curie Career Integration Grant PCIG13-GA-2013-618149 and HERMIONE (grant agreement 226354) within the 7th European Community Framework Programme, DOS MARES (CTM2007-66316-C02-01/MAR), GRACCIE-CONSOLIDER (CSD2007-00067), CASCADES (CTM2008-01334-E) and COSTEM (CTM2009-07806) projects. We are indebted to the crew and technicians of *BIO Hespérides*, *RV L'Atalante* and *BIO García del Cid* for their help in collecting the data. ^{210}Pb analysis of sediment samples was conducted at Laboratori de Radioactivitat Ambiental of the Universitat Autònoma de Barcelona (UAB). Lincoln Pratson and David Amblas are thanked for reviewing an earlier version of this manuscript. AM, MC, GL and XT belong to CRG on Marine Geociences, supported by grant 2009 SGR 1305, Generalitat de Catalunya.

References

Allen, S.E., Durrieu de Madron, X., 2009. A review of the role of submarine canyons in deep-ocean exchange with the shelf. Ocean Science 5, 607-620.

Alonso, B., Maldonado, A., 1990. Late Quaternary sedimentation patterns of the Ebro turbidite sytems (northwestern Mediterranean): Two styles of deep-sea deposition. Marine Geology 95, 353-377.

Alonso, B., Field, M.E., Gardner, J.M., Maldonado, A., 1990. Sedimentary evolution of the Pliocene and Pleistocene Ebro margin, northeastern Spain. Marine Geology 95, 265-288.

Amblas, D., Canals, M., Urgeles, R., Lastras, G., Liquete, C., Hughes-Clarke, J.E., Casamor, J.L., Calafat, A.M., 2006. Morphogenetic mesoscale analysis of the northeastern Iberian margin, NW Mediterranean Basin. Marine Geology 234, 3-20.

Amblas, D., Gerber, T.P., Canals, M., Pratson, L.F., Urgeles, R., Lastras, G., Calafat, A., 2011. Transient erosion in the Valencia Trough turbidite systems, NW Mediterranean Basin. Geomorphology 130, 173-184.

Amblas, D., Gerber, T.P., De Mol, B., Urgeles, R., Garcia-Castellanos, D., Canals, M., Pratson, L.F., Robb, N., Canning, J., 2012. The survival of a submarine canyon during long-term outbuilding of a continental margin. Geology 40, 543-546.

Antrobreh, A., Krastel, S., 2006. Morphology, seismic characteristics and development of Cap Timiris Canyon, offshore Mauritania: A newly discovered canyon preserved off a major arid climatic region. Marine and Petroleum Geology 23, 37-59.

Armitage, D.A., McHargue, T., Fildani, A., Graham, S.A., 2012. Post-avulsion channel evolution; Niger Delta continental slope. AAPG Bulletin 96, 823-843.

Babbonneau, N., Delacourt, C., Cancouet, R., Sisavath, E., Bachelery, P., Mazuel, A., Jorry, S.J., Deschamps, A., Ammann, J., Villeneuve, N., 2013. Direct sediment transfer from land to deep-sea: Insights into shallow multibeam bathmetry at La Réunion Island. Marine Geology 346, 47-57.

Baztan, J., Berné, S., Olivet, J.L., Rabineau, M., Aslanian, D., Gaudin, M., Réhault, J.P., Canals, M., 2005. Axial incision: The key to understand submarine canyon evolution (in the western Gulf of Lion). Marine and Petroleum Geology 22, 805-826.

Bertoni, C., Cartwright, J., 2005. 3D seismic analysis of slope-confined canyons from the Plio-Pleistocene of the Ebro Continental Margin (Western Mediterranean). Basin Research 17, 43-62.

Boltzmann, L., 1871. Einige allgemeine satze uber warmegleichgewicht. Wiener Berichte 63, 679-711.

Brothers, D.S., Ten Brink, U.S., Andrews, B.A., Chaytor, J.D., 2013a. Geomorphic characterization of the U.S. Atlantic continental margin. Marine Geology 338, 46-63.

Brothers, D.S., Ten Brink, U.S., Andrews, B.D., Chaytor, J.D., Twichell, D.C., 2013b. Geomorphic process fingerprints in submarine canyons. Marine Geology 337, 53-66.

Brunsden, D., Thornes, J.B., 1979. Landscape sensitivity and change. Transactions of the Institute of British Geographers 4, 463-484.

Burger, R.L., Fulthorpe, C.S., Austin, J.A., 2001. Late Pleistocene channel incisions in the southern Eel River basin, Northern California: Implications for tectonic vs. eustatic influences on shelf sedimentation patterns. Marine Geology 177, 317-330.

Cacchione, D.A., Drake, D.E., Losada, M.A., Medina, R., 1990. Bottom-boundary layer measurements on the continental shelf off the Ebro River, Spain. Marine Geology 95, 179-192.

Canals, M., Casamor, J.L., Urgeles, R., Lastras, G., Calafat, A.M., De Batist, M., Masson, D.G., Berné, S., Alonso, B., Hughes-Clarke, J.E., 2000. The Ebro Continental Margin, Western Mediterranean Sea: Interplay between canyon-channel systems and mass wasting processes. In: Nelson, C.H., Weimer, P. (Eds.), Deep-Water Reservoirs of the World: GCSSEPM Foundation 20th Annual Research Conference, Houston, USA, pp. 152-174.

Canals, M., Amblas, D., Lastras, G., Sànchez-Vidal, A., Calafat, A., Rayo, X., Casamor, J.L., 2012. Els canyons submarins, Història Natural dels Països Catalans: La Terra a l'Univers. Fundació Enciclopèdia Catalana, Barcelona, pp. 251-272.

Canals, M., Company, J.B., Martin, D., Sanchez-Vidal, A., Ramirez-Llodra, E., 2013. Integrated study of Mediterranean deep sea canyons: Novel results and future challenges. Progress in Oceanography 118, 1-27.

Canals, M., Puig, P., Durrieu de Madron, X., Heussner, S., Palanques, A., Fabres, J., 2006. Flushing submarine canyons. Nature 444, 354-357.

Cantelli, A., Paola, C., Parker, G., 2004. Experiments on upstream-migrating erosional narrowing and widening of an incisional channel caused by dam removal. Water Resources Research 40, W03304, doi:10.1029/2003WR002940.

Casas, D., Ercilla, G., Baraza, J., Alonso, B., Maldonado, A., 2003. Recent mass-movement processes on the Ebro continental slope (NW Mediterranean). Marine and Petroleum Geology 20, 445-457.

Clark, J.D., Pickering, K.T., 1996. Submarine Channels: Process and Architecture. Vallis Press, London.

Covault, J.A., Fildani, A., Romans, B.W., McHargue, T., 2011. The natural range of submarine canyon-and-channel longitudinal profiles. Geosphere 7, 313-332.

Covault, J.A., Shelef, E., Traer, M., Hubbard, S.M., Romans, B.W., Fildani, A., 2012. Deep-water channel run-out length: Insights from seafloor geomorphology. Journal of Sedimentary Research 82, 25-40.

Dade, W.B., 2001. Multiple scales in river basin morphology. American Journal of Science 301, 60-73.

Daly, R.A., 1936. Origin of submarine "canyons". American Journal of Science 31, 401-420.

Díaz, J.I., Nelson, C.H., Barber, J.H., Giró, S., 1990. Late Pleistocene and Holocene sedimentary facies on the Ebro continental shelf. Marine Geology 95, 333-352.

Díaz, J.I., Palanques, A., Nelson, C.H., Guillén, J., 1996. Morpho-structure and sedimentology of the Holocene Ebro prodelta mud belt (northwestern Mediterranean Sea). Continental Shelf Research 16, 435-456.

Emery, K.O., Uchupi, E., 1972. Western North Atlantic Ocean: Topography, Rocks, Structure, Water, Life and Sediments, Memoir 17, Tulsa.

Farrán, M., Maldonado, A., 1990. The Ebro continental shelf: Quaternary seismic stratigraphy and growth patterns. Marine Geology 95, 289-312.

Farre, J.A., McGregor, B.A., Ryan, W.B.F., Robb, J.M., 1983. Breaching the shelfbreak: Passage from youthful to mature phase in submarine canyon evolution. Society of Economic Paleontologists and Mineralogists, Special Publication 33, 25-39.

Felix, D.W., Gorsline, D.S., 1971. Newport submarine canyon, California: An example of the effects of shifting loci of sand supply upon canyon position. Marine Geology 10, 177-198.

Field, M.E., Gardner, J.V., 1990. Pliocene-Pleistocene growth of the Rio Ebro margin, northeast Spain: A prograding slope model. Geological Society of America Bulletin 102, 721-733.

Field, M.E., Gardner, J.V., Prior, D.B., 1999. Geometry and significance of stacked gullies on the northern California slope. Marine Geology 154, 271-286.

Fildani, A., Hubbard, S.M., Covault, J.A., Maier, K.L., Romans, B.W., Traer, M., Rowland, J.C., 2013. Erosion at inception of deep-sea channels. Marine and Petroleum Geology 41, 48-61.

Fildani, A., Normark, W.R., 2004. Late Quaternary evolution of channel and lobe complexes of Monterey Fan. Marine Geology 206, 199-223.

Fildani, A., Normark, W.R., Kostic, S., Parker, G., 2006. Channel formation by flow stripping: Large-scale scour features along the Monterey East Channel and their relation to sediment waves. Sedimentology 53, 1265-1287.

Font, J., Salat, J., Julià, A., 1990. Marine circulation along the Ebro continental margin. Marine Geology 95, 165-178.

Fryirs, K., Brierly, G.J., Erskine, W.D., 2012. Use of ergodic reasoning to reconstruct the historical range of variability and evolutionary trajectory of rivers. Earth Surface Processes and Landforms 37, 763-773.

Gee, M.J.R., Gawthorpe, R.L., Bakke, K., Friedmann, S.J., 2007. Seismic geomorphology and evolution of submarine channels from the Angolan continental margin. Journal of Sedimentary Research 77, 433-446.

Gerber, T.P., Amblas, D., Wolinsky, M.A., Pratson, L.F., Canals, M., 2009. A model for the long-profile shape of submarine canyons. Journal of Geophysical Research 114, F03002, doi: 10.1029/2008JF001190..

Glock, W.S., 1931. The development of drainage systems: A synoptic view. Geographical Review 21, 475-482.

Green, A.N., Goff, J.A., Uken, R., 2007. Geomorphological evidence for upslope canyon-forming processes on the northern KwaZulu-Natal shelf, SW Indian Ocean, South Africa. Geo-Marine Letters 27, 399-409.

Grünthal, G., Bosse, C., Sellami, S., Mayer-Rosa, D., Giardini, D., 1999. Compilations of the GSHAP regional seismic hazard for Europe, Africa and the Middle East. Annales Geophysicae 42, 1215-1223.

Guillén, J., Palanques, A., Puig, P., Durrieu de Madron, X., Nyffeler, F., 2000. Field calibrations of optical sensors for measuring suspended sediment concentration in the western Mediterranean. Scientia Marina 64, 427-435.

Hack, J.T., 1957. Studies of longitudinal stream profiles in Virginia and Maryland. US Geological Survey Professional Paper 294-B, 45-97.

Harris, P.T., Whiteway, T., 2011. Global distribution of large submarine canyons: Geomorphic differences between active and passive continental margins. Marine Geology 285, 69-86.

Heussner, S., Ratti, C., Carbonne, J., 1990. The PPS3 time-series sediment trap and the trap sample processing techniques used during the ECOMARGE experiment. Continental Shelf Research 10, 943-958.

Hilley, G.E., Arrowsmith, 2011. Geomorphic response to uplift along the Dragon's Back pressure ridge, Carrizo Plain, California. Geology 36, 367-370.

Huggett, R.J., 1998. Soil chronosequences, soil development and soil evolution: A critical review. Catena 32, 155-172.

Jobe, Z.R., Lower, D.R., Uchytil, S.J., 2011. Two fundamentally different types of submarine canyons along the continental margin of Equatorial Guinea. Marine and Petroleum Geology 28, 843-860.

Kertznus, V., Kneller, B., 2009. Clinoform quantification for assessing the effects of external forcing on continental margin development. Basin Research 21, 738-758.

Kirkbride, M., Matthews, D., 1997. The role of fluvial and glacial erosion in landscape evolution: The Ben Ohau Range, New Zealand. Earth Surface Processes and Landforms 22, 317-327.

Kneller, B., 2003. The influence of flow parameters on turbidite slope channel architecture. Marine and Petroleum Geology 20, 901-910.

Kostic, S., 2011. Modeling of submarine cyclic steps: Controls on their formation, migration, and architecture. Geosphere 7, 294-304.

Lambeck, K., Bard, E., 2000. Sea-level change along the French Mediterranean coast for the past 30000 years. Earth and Planetary Science Letters 175, 203-222.

Lastras, G., Acosta, J., Muñoz, A., Canals, M., 2011. Submarine canyon formation and evolution in the Argentine Continental Margin between 44°30'S and 48°S. Geomorphology 128, 116-136.

Lastras, G., Canals, M., Hughes-Clarke, J.E., Moreno, A., De Batist, M., Masson, D.G., Cochonat, P., 2002. Seafloor imagery from the BIG'95 debris flow, western Mediterranean. Geology 30, 871-874.

Laursen, J., Normark, W.R., 2002. Late Quaternary evolution of the San Antonio Submarine Canyon in the central Chile forearc (~33°S). Marine Geology 188, 365-390.

Leyland, J., Darby, S.E., 2008. An empirical–conceptual gully evolution model for channelled sea cliffs. Geomorphology 102, 419-434.

Li, X., Sun, Y., Mander, U., He, Y., 2011. Effects of land use intensity on soil nutrient distribution after reclamation in an estuary landscape. Landscape Ecology 28, 699-707.

Lo Iacono, C., Guillén, J., Puig, P., Ribó, M., Ballesteros, M., Palanques, A., Farrán, M., Acosta, J., 2010. Large-scale bedforms along a tideless outer shelf setting in the western Mediterranean. Continental Shelf Research 30, 1802-1813.

McGregor, B.A., Stubblefield, W.L., Ryan, W.B.F., Twichell, D.C., 1982. Wilmington submarine canyon: A marine fluvial-like system. Geology 10, 27-30.

Micallef, A., Mountjoy, J.J., 2011. A topographic signature of a hydrodynamic origin for submarine gullies. Geology 39, 115-118.

Migeon, S., Cattaneo, A., Hassoun, V., Larroque, C., Corradi, N., Fanucci, F., Dano, A., Mercier de Lepinay, B., Sage, F., Gorini, C., 2011. Morphology, distribution and origin of recent submarine landslides of the Ligurian Margin (North-western Mediterranean): Some insights into geohazard assessment. Mar Geophys Res 32, 225-243.

Mitchell, N.C., 2004. Form of submarine erosion from confluences in Atlantic USA continental slope canyons. American Journal of Science 304, 590-611.

Montgomery, D.R., Dietrich, W.E., 1992. Channel initiation and the problem of landscape scale. Science 255, 826-830.

Nelson, C.H., 1990. Estimated post-Messinian sediment supply and sedimenation rates on the Ebro continental margin. Marine Geology 95, 395-418.

Nittrouer, C.A., Sternberg, R.W., Carpenter, R., Bennett, J.T., 1979. The use of Pb-210 geochronology as a sedimentological tool: application to the Washington continental shelf. Marine Geology 31, 297-316.

Normark, W.R., Carlson, P.R., 2003. Giant submarine canyons: Is size any clue to their importance in the rock record? Geological Society of America Special Paper 370, 175-190.

Normark, W.R., Piper, D.J.W., 1968. Deep-sea fan valleys, past and present. Geological Society of America Bulletin 80, 1859-1866.

Normark, W.R., Piper, D.J.W., 1991. Initiation processes and flow evolution of turbidity currents: Implications for the depositional record. In: Osborne, R.E. (Ed.), From Shoreline to Abyss: Contributioons in Marine Geology in Honor of Francis Parker Shepard, pp. 207-230.

Normark, W.R., Paull, C.K., Caress, D.W., Sliter, R., 2009. Fine-scale relief related to Late Holocene channel shifting within the floor of the upper Redondo Fan, offshore southern California. Sedimentology 56, 1670-1689.

Obanawa, H., Hayakawa, Y.S., Matsukura, Y., 2009. Rates of slope decline, talus growth and cliff retreat along the Shomyo River in central Japan: A space-time substitution approach. Geografiska Annaler 91, 269-278.

Obelcz, J., Brothers, D., Chaytor, J.D., ten Brink, U.S., Ross, S.W., Brooke, S., in press. Geomorphic characterization of four shelf-sourced submarine canyons along the U.S. Mid-Atlantic continental margin. Deep-Sea research Part II.

Orange, D.L., Anderson, R.S., Breen, N.A., 1994. Regular canyon spacing in the submarine environment: The link between hydrology and geomorphology. GSA Today 4(29), 36-39.

Paine, D.M., 1985. 'Ergodic' reasoning in geomorphology: Time for a review of the term? Progress in Physical Geography 9, 1-15.

Palanques, A., Plana, F., Maldonado, A., 1990. Recent influence of man on the Ebro margin ssedimentation system, northwestern Mediterranean Sea. Marine Geology 95, 247-273.

Palanques, A., Puig, P., Guillén, J., Jiménez, J., Gracia, V., Sànchez-Arcilla, A., Madsen, O., 2002. Near-bottom suspended sediment fluxes on the microtidal low-energy Ebro continental shelf (NW Mediterranean). Continental Shelf Research 22, 285-303.

Parker, G., Izumi, N., 2000. Purely erosional cyclic and solitary steps created by flow over a cohesive bed. Journal of Fluid Mechanics 419, 203-238.

Parsons, J.D., Friedrichs, C.T., Mohrig, D., Traykovski, P., Imran, J., Syvitski, J.P., Parker, G., Puig, P., Buttles, J., Garcia, M.H., 2006. The mechanics of marine sediment gravity flows. In: C.A. Nittrouer, J.A. Austin, M. Field, M.S. Steckler, J.P. Syvitski, P.L. Wiberg (Eds.), Continental Margin Sedimentation: From Sediment Transport to Sequence Stratigraphy. Blackwell Publishing, Oxford, pp. 275-338.

Paull, C.K., Ussler, W., Greene, H.G., Keaten, R., Mitts, P., Barry, J., 2003. Caught in the act: The 20 December 2001 gravity flow event in Monterey Canyon. Geo-Marine Letters 22, 227-232.

Paull, C.K., Ussler, W., Greene, H.G., Keaten, R., Mitts, P., Barry, J., 2003. Caught in the act: The 20 December 2001 gravity flow event in Monterey Canyon. Geo-Marine Letters 22, Paull, C.K., Mitts, P., Ussler, W., Keaten, R., Greene, H.G., 2005. Train of sand in the upper Monterey Canyon. Geological Society of America Bulletin 117, 1134-1145.

227-232.

Paull, C.K., Caress, D.W., Lundsten, E., Gwiazda, R., Anderson, K., McGann, M., Conrad, J., Edwards, B., Sumner, E.J., 2013. Anatomy of the La Jolla Submarine Canyon system; offshore southern California. Marine Geology 335, 16-34.

Perron, J.T., Dietrich, W.E., Kirchner, J.W., 2008. Controls on the spacing of first-order valleys. Journal of Geophysical Research 113, F04016, doi:10.1029/2007JF000977..

Perron, J.T., Kirchner, J.W., Dietrich, W.E., 2009. Formation of evenly spaced ridges and valleys. Nature 460, 502-505.

Pickett, S.T.A., 1989. Space-for-time substitution as an alternative to long term studies. In: Likens, G.E. (Ed.), Long-Term Studies in Ecology. Springer-Verlag, New York, pp. 110-135.

Piper, D.J.W., Normark, W.R., 2009. Processes that initiate turbidity currents and their influence on turbidites: A marine geology perspective. Journal of Sedimentary Research 79, 347-362.

Pirmez, C., Beaubouef, R.T., Friedmann, S.J., Mohrig, D.C., 2000. Equilibrium profile and baselevel in submarine channels: Examples from Late Pleistocene systems and implications for the architecture of deep water reservoirs. In: Weimar, P., Slatt, R.M., Coleman, J.M., Rosen, N.C., Nelson, H., Bouma, A.H., Styzen, M.J., Lawrence, D.T. (Eds.), Deep Water Reservoirs of the World. GCSSEPM Foundation 20th Annual Research Conference, pp. 782-805.

Pirmez, C., Imran, J., 2003. Reconstruction of turbidity currents in Amazon channel. Marine and Petroleum Geology 20, 823-849.

Popescu, I., Lericolais, G., Panin, N., Normand, A., Dinu, C., Le Drezen, É., 2004. The Danube submarine canyon (Black Sea): Morphology and sedimentary processes. Marine Geology 206, 249-265.

Posamentier, H.W., Jervey, M.T., Vail, P.R., 1988. Eustatic controls on clastic deposition, I. Conceptual framework. In: Wilgus, C.K., Hastings, B.S., Kendall, M.A., Posamentier, H.W., Ross, C.A., Van Wagoner, J.C. (Eds.), Sea Level Changes – An Integrated Approach. SEPM Special Publication No. 42, pp. 125-154.

Pratson, L.F., Coakley, B.J., 1996. A model for the headward erosion of submarine canyons induced by downslope-eroding sediment flows. Geological Society of America Bulletin 108, 225-234.

Pratson, L.F., Ryan, W.B.F., Mountain, G.S., Twichell, D.C., 1994. Submarine canyon initiation by downslope-eroding sediment flows: Evidence in late Cenozoic strata on the New Jersey continental slope. Geological Society of America Bulletin 106, 395-412.

Pratson, L.F., Nittrouer, C.A., Wiberg, P.L., Steckler, M.S., Swenson, J.B., Cacchione, D.A., Karson, J.A., Murray, A.B., Wolinsky, M.A., Gerber, T.P., Mullenbach, B.L., Spinelli, G.A., Fulthorpe, C.S., O'Grady, D.B., Parker, G., Driscoll, N.W., Burger, R.L., Paola, C., Orange, D.L., Field, M.E., Friedrichs, C.T., Fedele, J.J., 2009. Seascape evolution on clastic continenal shelves and slopes. In: C.A. Nitrouer, J.A. Austin, M.E. Field, J.H. Kravitz, J.P.M. Syvitski, P.L. Wiberg (Eds.), Continental Margin Sedimentation: From Sediment Transport to Sequence Stratigraphy: IAP Special Publication. Blackwell Publishing, Oxford, pp. 339-380.

Puertos del Estado, 2013. Extremos Máximos de oleaje (Altura Significante), Boya de Valencia, Periodo 2005-2012.

Puig, P., Palanques, A., Guillén, J., 2001. Near-bottom suspended sediment variability caused by storms and near-inertial internal waves in the Ebro mid continental shelf (NW Mediterranean). Marine Geology 178, 81-93.

Puig, P., Ogston, A.S., Mullenbach, B.L., Nittrouer, C.A., Parson, J.D., Sternberg, R.W., 2004. Storm-induced sediment gravity flows at the head of the Eel submarine canyon, northern California margin. Journal of Geophysical Research 109, C03019, doi:10.1029/2003JC001918..

Puig, P., Palanques, A., Orange, D., Lastras, G., Canals, M., 2008. Dense shelf water cascades and sedimentary furrow formation in the Cap de Creus Canyon, northwestern Mediterranean Sea. Continental Shelf Research 28, 2017-2030.

Puig, P., Palanques, A., Martín, J., 2014. Contemporary sediment-transport processes in submarine canyons. Annual Review of Marine Science 6, 53-77.

Ribó, M., Puig, P., Palanques, A., Lo Iacono, C., 2011. Dense shelf water cascades in the Cap de Creus and Palamós submarine canyons during winters 2007 and 2008. Marine Geology 284, 175-188.

Rigon, R., Rodríguez-Iturbe, I., Maritan, A., Giacometti, A., Tarboton, D.G., Rinaldo, A., 1996. On Hack's Law. Water Resources Research 32, 3367-3374.

Rinaldo, A., Rodriguez-Iturbe, I., Rigon, R., Bras, R.L., Ijjasz-Vasquez, E., Marani, A., 1992. Minimum energy and fractal structures of drainage networks. Water Resources Research 28, 2183-2195.

Sanchez-Cabeza, J.A., Masqué, P., Ani-Ragolta, I., 1998. ^{210}Pb and ^{210}Po analysis in sediments and soils by microwave acid digestion. Journal of Radioanalytical and Nuclear Chemistry 227, 19-22.

Sànchez-Vidal, A., Canals, M., Calafat, A., Lastras, G., Pedrosa-Pàmies, R., Menéndez, M., Medina, R., Company, J.B., Hereu, B., Romero, J., Alcoverro, T., 2012. Impacts on the deep-sea ecosystem by a severe coastal storm. PLoS ONE 7, e30395, doi:10.1371/journal.pone.0030395.

Schmidt, K.H., Meitz, P., 2000. Effects of increasing humidity on slope geomorphology: Cuesta scarps on the Colorado Plateau, USA, The Hydrology-Geomorphology Interface: Rainfall, Floods, Sedimentation, Land Use, Jerusalem, pp. 165-181.

Schumm, S.A., Harvey, M.D., Watson, C.C., 1984. Incised Channels: Morphology, Dynamics and Control. Water Resources Publications, Chelsea, Michigan.

Shepard, F.P., 1981. Submarine canyons: Multiple causes and long-time persistence. American Association of Petroleum Geologists Bulletin 65, 1062-1077.

Shepard, F.P., Buffington, E.C., 1968. La Jolla submarine fan-valley. Marine Geology 6, 107-143.

Shepard, F.P., Dill, R.F., 1966. Sumbarine Canyons and Other Sea Valleys. Rang McNally, Chicago.

Simon, A., Hupp, C.R., 1986. Channel evolution in modified Tennessee channels, Proceedings of the Fourth Federal Interagency Sedimentation Conference. US Government Printing Office, Washington D.C., pp. 71-82.

Stanley, D.J., Nelsen, T.A., Stuckenrath, R., 1984. Recent sedimentation on the New Jersey slope and rise. Science 226, 125-133.

Stolar, D.B., Willett, S.D., Montgomery, D.R., 2007. Characterization of topographic steady state in Taiwan. Earth and Planetary Science Letters 261, 421-431.

Strahler, A.N., 1952. Hypsometric (area-altitude) analysis of erosional topography. Geological Society of America Bulletin 63, 1117-1142.

Sultan, N., Gaudin, M., Berne, S., Canals, M., Urgeles, R., Lafuerza, S., 2007. Analysis of slope failure in submarine canyon heads: An example from the Gulf of Lions. Journal of Geophysical Research 112, F01009, doi:10.1029/2005JF000408.

Twichell, D.C., Knebel, H.J., Folger, D.W., 1977. Delaware river: Evidence for its former extension to Wilmington submarine canyon. Science 195, 483-485.

Twichell, D.C., Roberts, D.G., 1982. Morphology, distribution and development of submarine canyons on the United States Atlantic continental slope between Hudson and Baltimore Canyons. Geology 10, 408-412.

Urgeles, R., Camerlenghi, A., Garcia-Castellanos, D., De Mol, B., Garces, M., Verges, J., Haslam, I., Hardman, M., 2011. New contraints on the Messinian sealevel drawdown from 3D seismic data of the Ebro Margin, western Mediterranean. Basin Research 23, 123-145.

Vachtman, D., Mitchell, N.C., Gawthorpe, B., 2013. Morphologic signatures in submarine canyons and gullies, central USA Atlantic continental margins. Marine and Petroleum Geology 41, 250-263.

Vail, P.R., Mitchum, R.M., Thompson, S., 1977. Seismic stratigraphy and global changes of sea level; Part 4, Global cycles of relative changes of sea level. In: Payton, C.E. (Ed.), Memoir: American Association of Petroleum Geologists, pp. 83-97.

Wright, L.D., 1995. Morphodynamics of Inner Continental Shelves. CRC Press, Boca Raton, FL.

Zúñiga, D., Mar Flexas, M., Sanchez-Vidal, A., Coenjaerts, J., Calafat, A., Jordà, G., García-Orellana, J., Puigdefàbregas, J., Canals, M., Espino, M., Sardà, F., Company, J.B., 2009.

Particle fluxes dynamics in Blanes submarine canyon (Northwestern Mediterranean). Progress in Oceanography 82, 239-251.

Table captions

Table 1. List and description of morphometric parameters extracted from features 1 – 6.

Table 1:

Morphometric parameter	Description
Thalweg length	Distance along valley axis from head to terminus
Linear length	Straight line distance between valley head and terminus
Width	Maximum distance between valley rims, measured perpendicularly to the valley axis
Valley depth	Maximum vertical distance between valley rims and floor
Area	Measured for a smooth surface interpolated across the valley boundaries
Volume	Measured by subtracting the original bathymetry from a smooth surface interpolated across the valley boundaries; the difference in bathymetry at each point is multiplied by the cell area and the values are summed
Valley axial slope gradient	Measured by dividing the difference in bathymetric depth at the canyon head and terminus, and dividing by thalweg length
Profile concavity index	Change in axial slope gradient with distance along thalweg
Total number and thalweg length of valleys and tributaries	-
Drainage density	Total thalweg length of valleys and tributaries divided by 'Area'
Upslope and downslope elongation	Change in thalweg length upslope/downslope of valley head/terminus between consecutive features
Volume of material eroded	Change in volume upslope/downslope of valley head/terminus between consecutive features
Bifurcation ratio	Ratio of the number of valleys of any order to the number of valleys of the next highest order; the Strahler stream order is used (Strahler, 1952)

Figure captions

Fig. 1. Location of study area. (A) Location map of the Ebro Margin, western Mediterranean Sea. (B) Bathymetric map of the Ebro Margin (isobaths every 100 m). The sea-level during the Last Glacial Maximum (LGM) is denoted by a bold isobath (Lambeck and Bard, 2000). The location of Columbretes Islets (CI) is also indicated.

Fig. 2. Bathymetric and isobath map (100 m intervals) of the south Ebro Margin. The location of the figure is shown in Fig. 1. M1 and M2 indicate the location of moorings 1 and 2, respectively. NCC = North Columbretes Canyon; SCC = South Columbretes Canyon.

Fig. 3. Gullies and canyons within the study area. (A) Bathymetric and shaded relief map of 18 gullies and canyons incising the south Ebro Margin. Location is shown in Fig. 2. Five gullies and canyons considered in this study are outlined in solid black and labelled 1–5. The location of the outer shelf sand body, interpreted as palaeo-delta deposits, is marked (Díaz et al., 1990; Lo Iacono et al., 2010). 'M2' indicates the location of mooring 2. The location of valleys 'X-Z' is indicated (see main text). (B) Backscatter imagery of the seabed shown in Fig. A. Numbers in squares denote feature numbers.

Fig. 4. Canyon-channel system within the study area. (A) Bathymetric and shaded relief map of the canyon-channel system (feature 6). Location is shown in Fig. 2. The location of the outer shelf sand body, interpreted as palaeo-delta deposits, is marked (Díaz et al., 1990; Lo Iacono et

al., 2010). 'M1' indicates the location of mooring 1. (B) Backscatter imagery of the seabed shown in A. The number in squares denote the feature number.

Fig. 5. Schematics showing the morphometric parameters measured from the bathymetric data from the study area (Covault et al., 2012).

Fig. 6. Time series of in situ current speed (cm s^{-1}), suspended sediment concentration (*SSC*) (mg l^{-1}) and cumulative transport (T m^{-2}) recorded for mooring M1 in feature 6 for the time period October 2008 to January 2009 (A–C), and for mooring M2 in feature 5 for the time period from May 2010 to June 2011 (D–F). The time series of sediment flux (g m^{-2} d^{-1}) for mooring M2 for the time period from May 2010 to June 2011 is shown in G. No downward particle flux data were recorded from mooring M1 in feature 6.

Fig. 7. Selected valleys and their mapped network of tributaries ordered according to increasing length. Isobaths are used as reference points to locate valleys with respect to each other. Numbers in squares denote feature numbers.

Fig. 8. Different types of valley morphologies. (A) Slope gradient map draped on shaded relief map showing the interpreted erosional morphologies in feature 5. 'M2' indicates the location of mooring 2. (B) Shaded relief map of shallow and narrow elongate depressions connecting the outer shelf sand body, interpreted as a palaeo-delta deposit, with the head of the valley in feature 5. (C) Bathymetric and shaded relief map of the mouth of feature 5, showing asymmetric scours interpreted as cyclic steps. (D) Bathymetric and shaded relief of the lower reaches of the valley

in feature 6, displaying a hanging ox-bow, levées, terraces and a sinuous channel course (isobaths at 10 m intervals). Numbers in squares denote feature numbers.

Fig. 9. Longitudinal downslope and valley depth profile plots. (A) Valley downslope profiles and concavity index (underlined). (B) Variation of valley incised depth with distance from shelf break, measured along the thalweg, in features 1–5. (C) Variation of valley incised depth with distance from shelf break, measured along the thalweg, in feature 6. (D) Convex–concave downslope profile of canyon X (see main text), the location of which is denoted in Fig. 3A. Numbers in squares denote feature numbers.

Fig. 10. Plots of variation of the following morphometric attributes with thalweg length for each feature: (A) Width and depth; (B) Width:depth ratio; (C) Area and volume; (D) Axial slope gradient and drainage density; (E) Upslope and downslope elongation between consecutive features; (F) Volume of material eroded upslope and downslope of valley between consecutive features; (G) Total number and thalweg length of valleys. Numbers in squares denote feature numbers.

Fig. 11. Valley morphometrics bivariate plots. (A) Plot of variation of valley length with valley area; a power law trendline is fitted for the first five features. (B) Plot of trendlines of the variation of slope gradient and stream length with stream order (Strahler, 1952) for each feature; all trendlines are associated with an R^2 value higher than 0.6. (C) Plot of variation of valley width with valley length; a linear trendline is fitted for the first five features. (D) Plot of variation of profile concavity with valley length. Numbers in squares denote feature numbers.

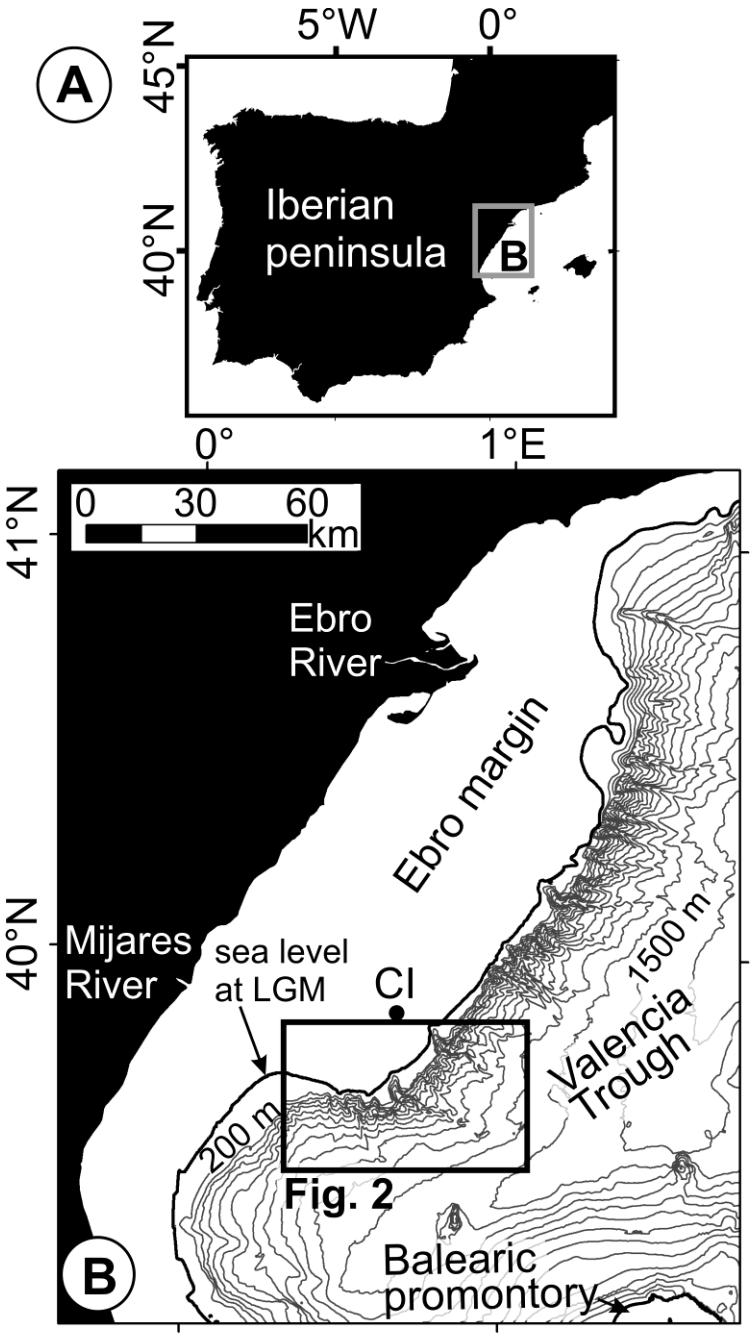

Figure 1

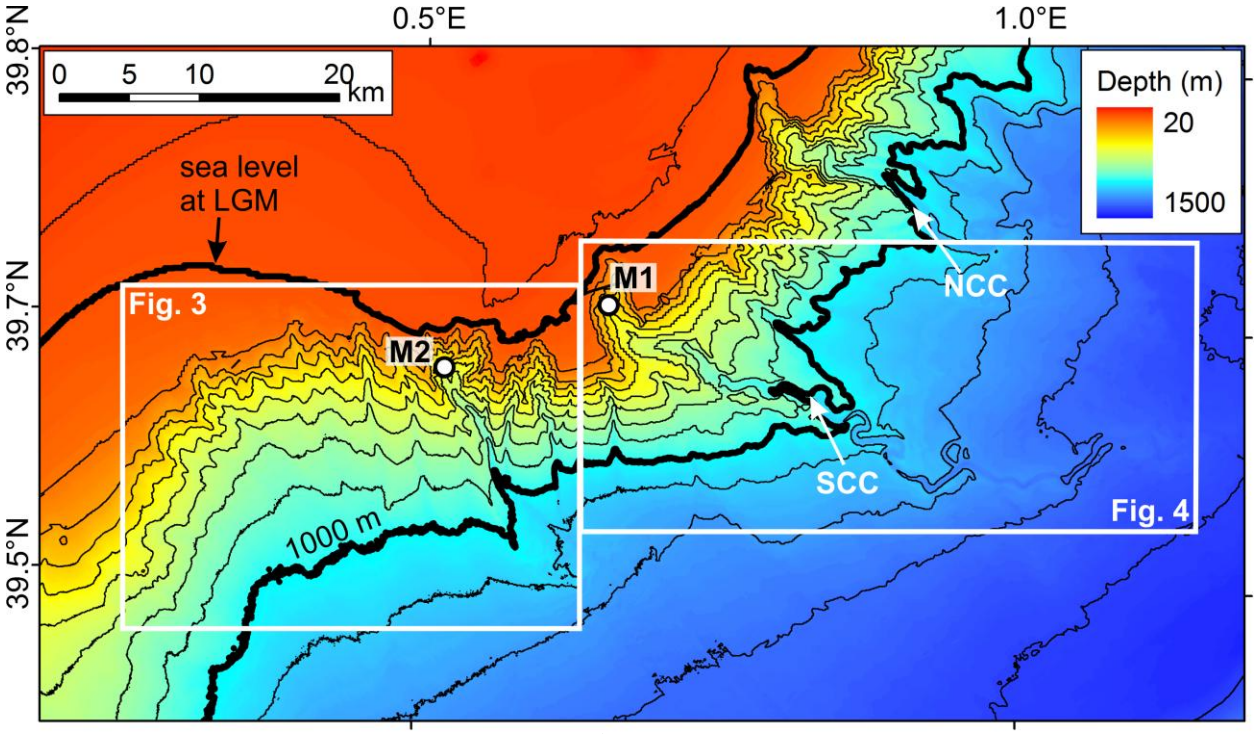

Figure 2

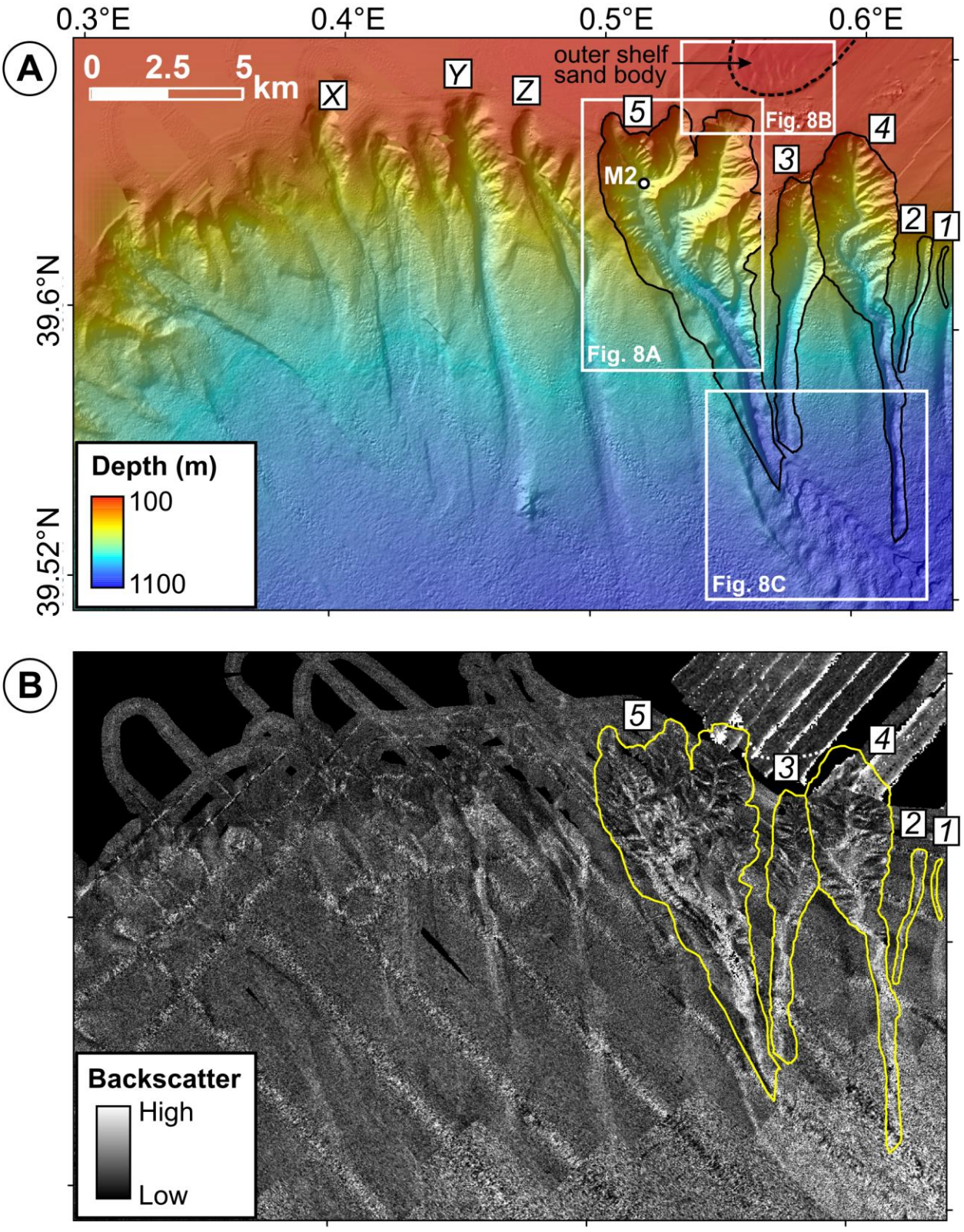
A
0.3°E
0.4°E
0.5°E
0.6°E
39.6°N
39.52°N
0 2.5 5 km
X
Y
Z
outer shelf sand body
Fig. 8B
5
4
3
2
1
M2
Fig. 8A
Fig. 8C
Depth (m)
100
1100
B
Backscatter
High
Low

Figure 3

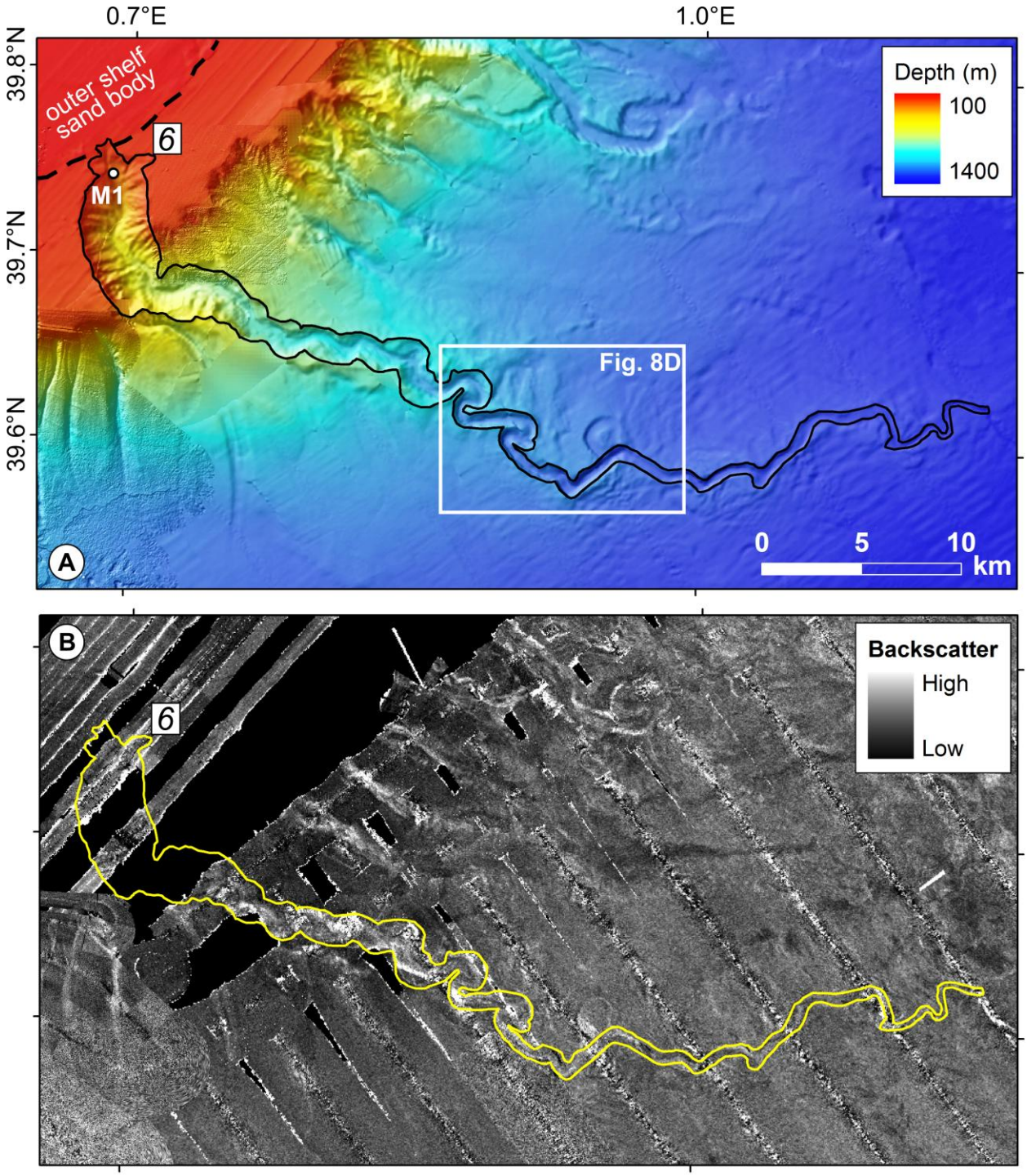

Figure 4

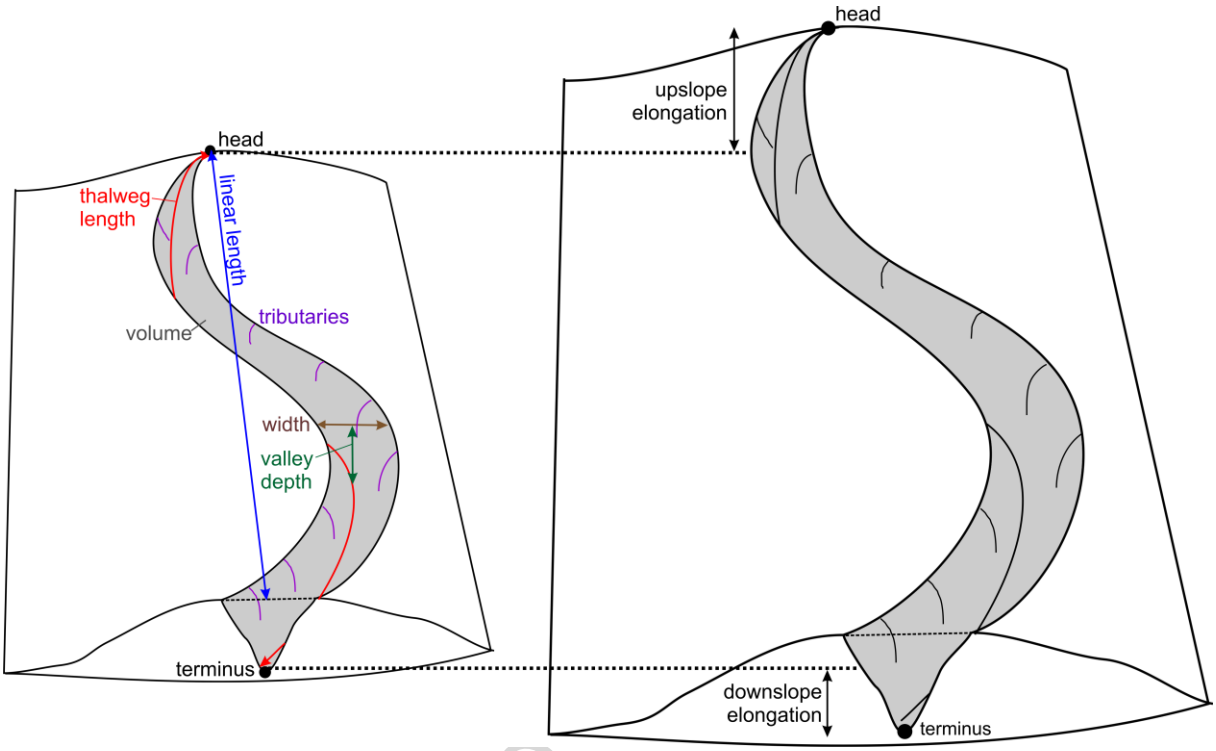

Figure 5

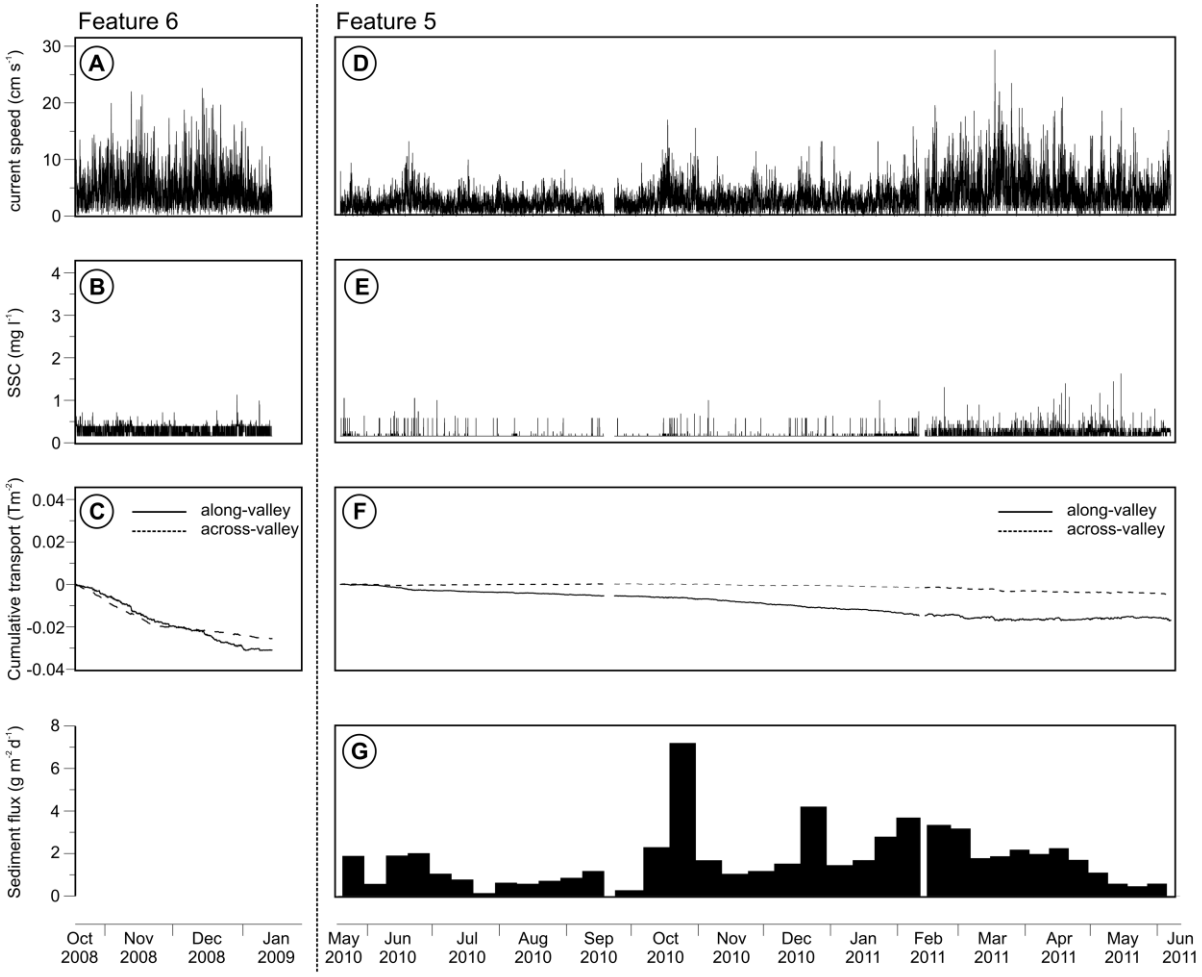

Figure 6

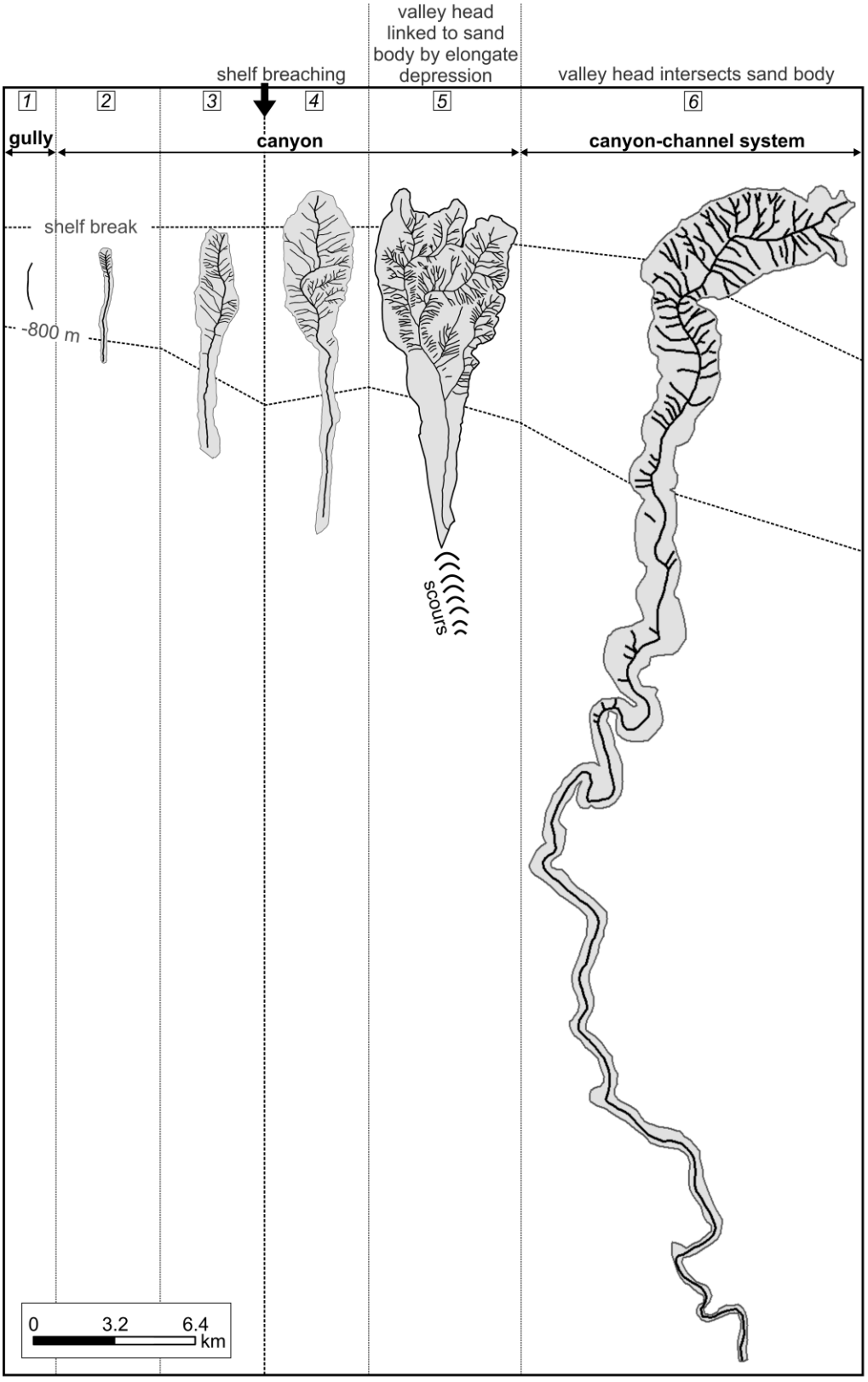

Figure 7

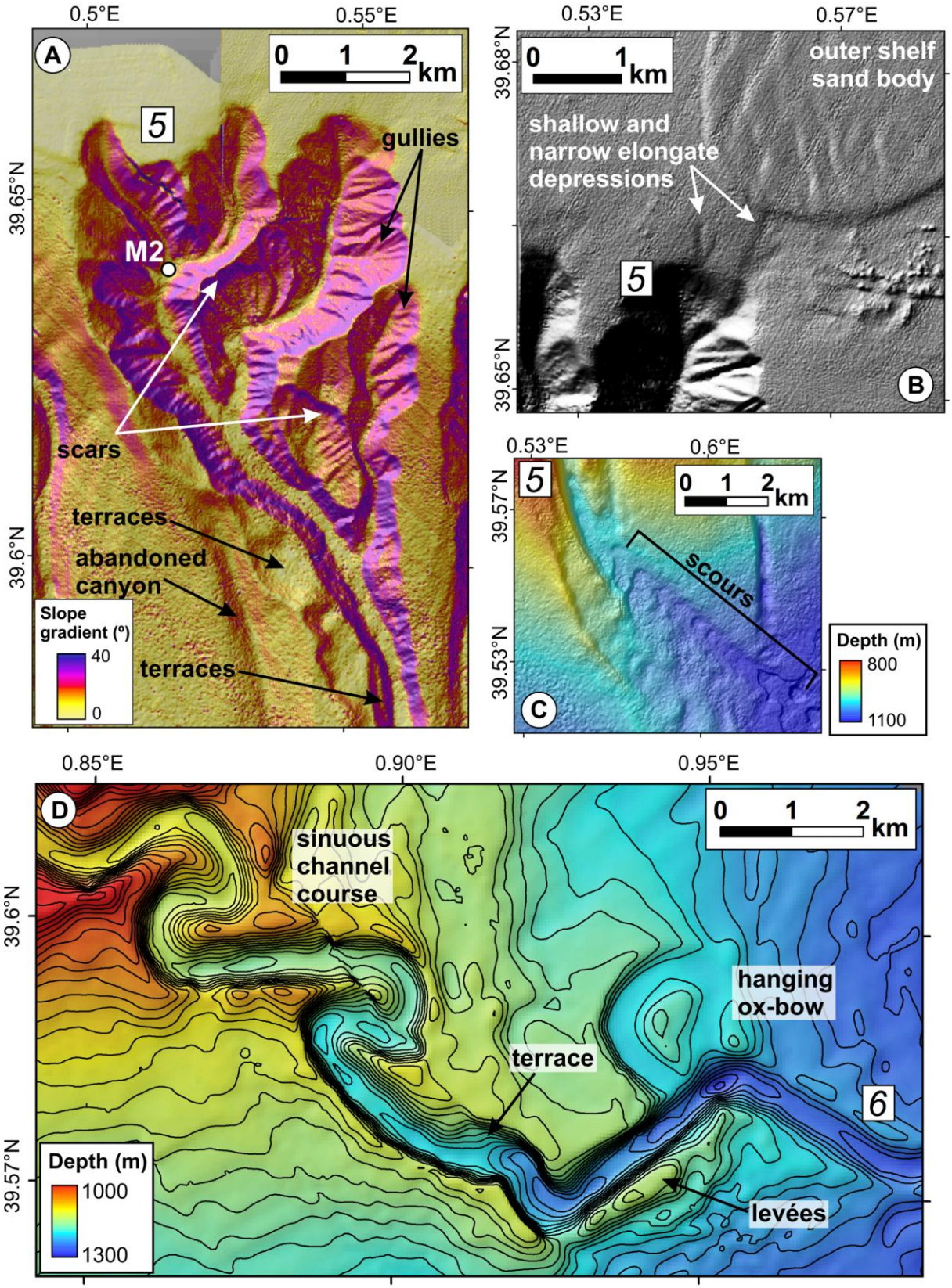
A
0.5°E
0.55°E
39.65°N
39.6°N
0 1 2 km
5
gullies
M2
scars
terraces
abandoned canyon
terraces
Slope gradient (°)
40
0
B
0.53°E
0.57°E
39.68°N
39.65°N
0 1 km
outer shelf sand body
shallow and narrow elongate depressions
5
C
0.53°E
0.6°E
39.57°N
39.53°N
5
0 1 2 km
scours
Depth (m)
800
1100
D
0.85°E
0.90°E
0.95°E
39.6°N
39.57°N
0 1 2 km
sinuous channel course
hanging ox-bow
terrace
6
levées
Depth (m)
1000
1300

Figure 8

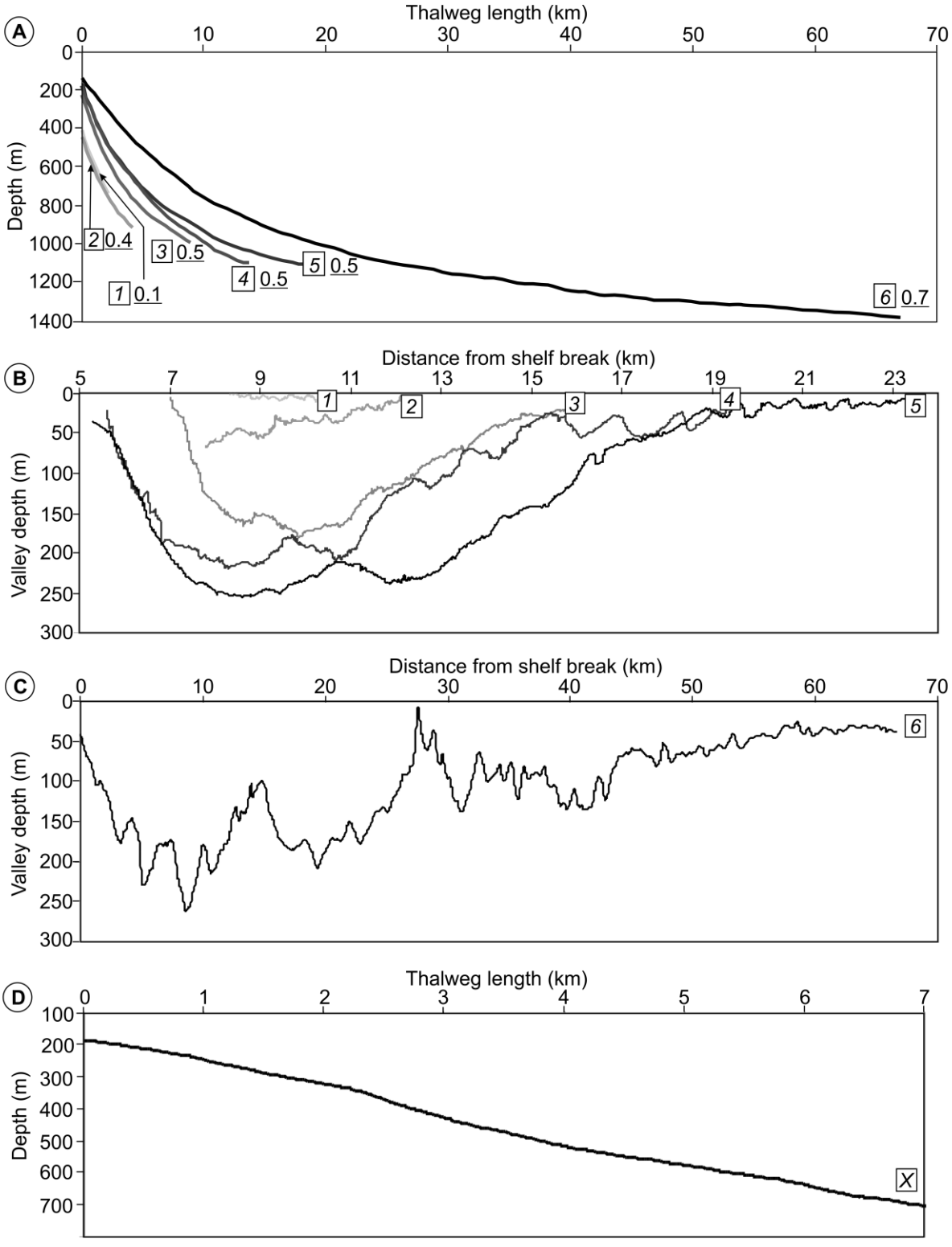

Figure 9

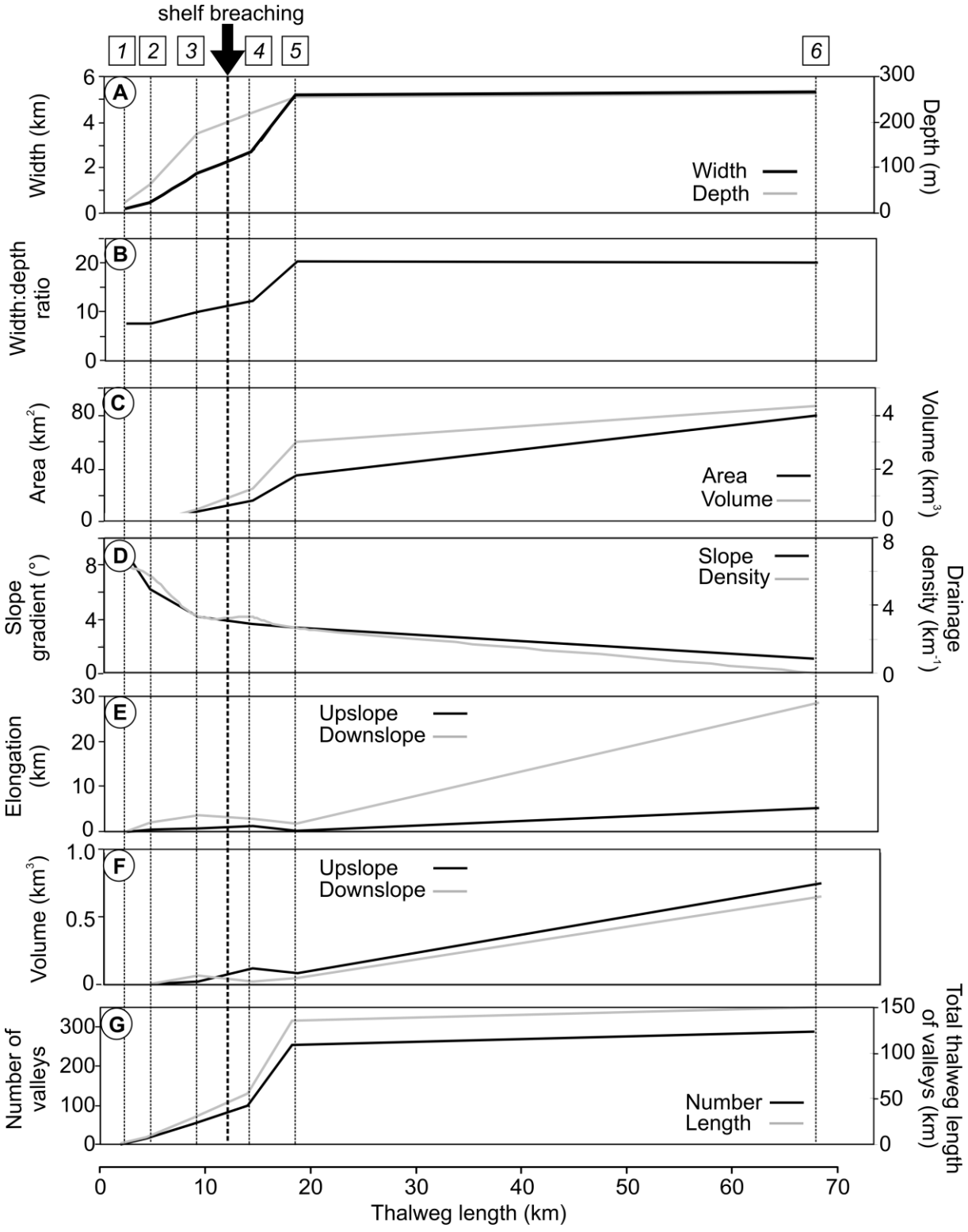

Figure 10

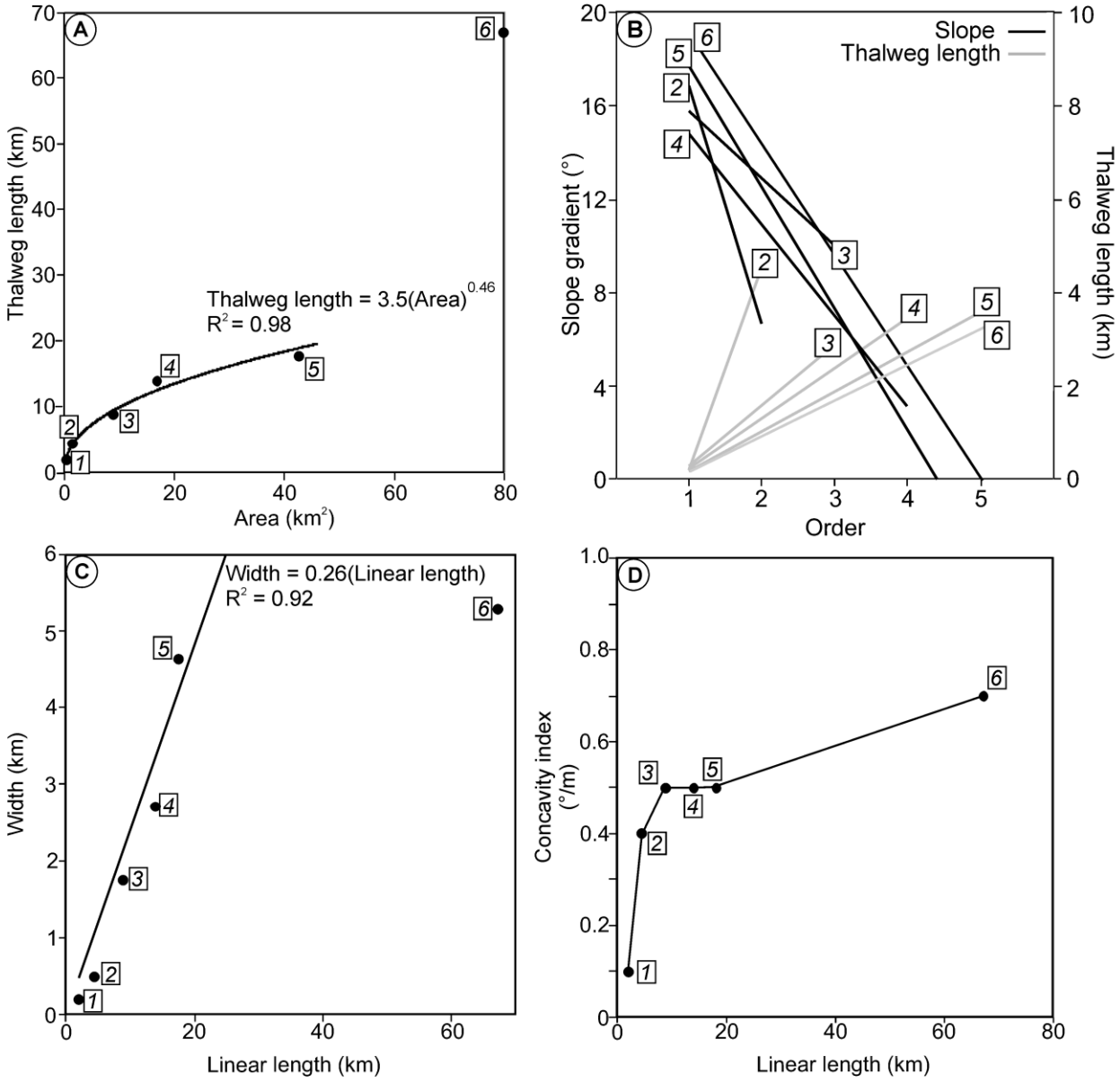

Figure 11

Highlights

- We analyse multibeam data and in situ measurements from south Ebro Margin
- Space-for-time substitution concept is tested in a passive progradational margin
- Concept can be used to reconstruct evolution of a submarine canyon-channel system
- Morphometry provides new insights into morphological evolution of submarine canyons